VOTE 71911

MATHEMATICAL MODELLING OF MASS TRANSFER IN MULTI-STAGE ROTATING DISC CONTACTOR COLUMN

(PEMODELAN MATEMATIK BAGI PERALIHAN JISIM DALAM TURUS PENGEKSTRAKAN CAKERA BERPUTAR MULTI-TINGKAT)

KHAIRIL ANUAR ARSHAD
JAMALLUDIN TALIB
NORMAH MAAN

RESEARCH VOTE NO: 71911

Faculty of Science
Universiti Teknologi Malaysia

JUNE 2006

ABSTRACT

(Keywords:Mass Transfer, RDC Column, Quadratic Driving Force, Forward Model)

In this study, the development of an improved forward model for the mass transfer process in the Rotating Disc Contactor (RDC) column was carried out. The existing mass transfer model with constant boundary condition does not accurately represent the mass transfer process. Thus, a time-varying boundary condition was formulated and consequently the *new fractional approach to equilibrium* was derived. This derivation initiated the formulation of the modified quadratic driving force, called *Time-dependent Quadratic Driving Force (TQDF)*. Based on this formulation, a Mass Transfer of A Single Drop (MTASD) Algorithm was designed, followed by a more realistic Mass Transfer of Multiple Drops (MTMD) Algorithm which was later refined to become another algorithm named the Mass Transfer Steady State (MTSS) Algorithm. The improved forward models, consisting of a system of multivariate equations, successfully calculate the amount of mass transfer from the continuous phase to the dispersed phase and was validated by the simulation results.

Key Researchers:

Associate Professor Dr Khairil Anuar Arshad(Head)

Associate Professor Dr Jamalludin Talib

Dr Normah Maan

E-mail:khairil@mel.fs.utm.my

Tel no:07-5534385

Vote no:71911

ABSTRAK

Dalam kajian ini, pembentukan model ke depan yang lebih baik dan model songsangan bagi proses peralihan jisim di dalam Turus Pengekstrakan Cakera Berputar (RDC) telah dijalankan. Model yang sedia ada dengan syarat sempadan tetap tidak mewakili proses peralihan jisim dengan tepat. Dengan itu, syarat sempadan yang merupakan suatu fungsi masa berubah telah dirumuskan dan seterusnya *pendekatan pecahan untuk keseimbangan* yang baru diterbitkan. Penerbitan ini telah memulakan perumusan daya pacu kuadratik ubahsuai, yang dipanggil *daya pacu kuadratik bersandaran masa (TQDF)*. Berdasarkan perumusan ini, satu Algoritma Peralihan Jisim untuk Sebutir Titisan (MTASD) telah direkabentuk , diikuti oleh satu algoritma yang lebih realistik algoritma Peralihan Jisim untuk Multi Titisan (MTMD) yang mana kemudiannya, telah diperbaiki dan dinamakan Algoritma Peralihan Jisim Berkeadaan Mantap (MTSS).

TABLE OF CONTENTS

LIST OF TABLES

LIST OF FIGURES

LIST OF SYMBOLS/NOTATIONS

a	-	radius of a sphere
A	-	Column cross sectional area (m^2)
C	-	Concentration (kg/m^3)
d	-	Drop diameter (m)
d_c	-	Column diameter (m)
d_{cr}	-	Critical drop diameter for breakage (m)
d_{max}	-	Maximum stable drop diameter (m)
d_o	-	Initial drop diameter (m)
d_{32}	-	Sauter mean drop size (m)
d_{av}	-	Average diameter of drop (m)
D_c	-	Molecular diffusivity in continuous phase (m^2/s)
D_d	-	Molecular diffusivity in dispersed phase (m^2/s)
D_e	-	Eddy diffusivity (m^2/s)
D_{oe}	-	Overall effective diffusivity (m^2/s)
D_r	-	Rotor diameter (m)
D_s	-	Stator diameter (m)
e	-	Back-flow ratio
E	-	Power consumption per unit mass (Eq. (2.9)) (w/kg)
E_{am}	-	Axial mixing coefficient (m^2/s)
E_c	-	Continuous phase axial mixing coefficient (m^2/s)
E_o	-	Eotvos number
F_d	-	Flowrate of dispersed (cm^3/s)
fr	-	Fraction of daughter drop
g	-	Acceleration due to gravity (m^2/s)
g_i	-	Dynamic volume fraction of drops with size d_i
h	-	Height of column (m)
h_c	-	Height of an element of compartment (m)
H	-	Column height (m)
k_d	-	Drop film mass transfer coefficient (m/s)
K_{od_i}	-	Overall dispersed phase based mass transfer coefficient for drop with size d_i (m/s)
m	-	Exponent in the equation of slip velocity
M	-	Morton number in terminal velocity
N_r	-	Rotor speed (s^{-1})
N_{cr}	-	Critical rotor speed for drop breakage (s_{-1})
N_{cl}	-	Number of classes

N_{st}	-	Number of stages
P	-	Probability of breakage
P_R	-	Power consumption per disc (w/m^3)
Re	-	Drop Reynolds number
Re_k	-	Drop Reynolds number using V_k
$Re_{D,\omega}$	-	Disc Reynolds number based on angular velocity
Sc	-	Schmidt number
Sh	-	Sherwood number
$t_{r,i}$	-	Resident time of drops with size d_i in a stage (s)
V	-	Drop volume (m^3)
V_c	-	Continuous phase superficial velocity (m/s)
V_d	-	Dispersed phase superficial velocity (m/s)
V_k	-	Drop characteristic velocity (m/s)
V_s	-	Slip velocity (m/s)
V_t	-	Drop terminal velocity (m/s)
We	-	Weber number for drop
$We_{D,\omega}$	-	Disc angular Weber number
x_m	-	Mean number of daughter drops
X	-	Hold-up

Greek symbols

Φ	-	Equilibrium curve slope $(dC_d/dC_c$
γ	-	Interfacial tension (N/m)
β_n	-	Eigenvalues
μ_c, μ_d	-	Continuous and dispersed phase viscosities $(mPas)$
ρ_c, ρ_d	-	Continuous and dispersed phase densities (kg/m^3)
$\Delta\rho$	-	densities differences (kg/m^3)
κ	-	Viscosity ratio
ω	-	Angular velocity (s^1)
ω_{cr}	-	Critical angular velocity (s^1)

Supercripts

$*$	-	dimensional variables
$'$	-	differentiation with respect to $\overline{\eta}$
s	-	denotes steady part of the solution
u	-	denotes unsteady part of the solution

Subcripts

c, d	-	Continuous and dispersed phase
i	-	drop size classes
n	-	Stage number
av	-	average value

LIST OF APPENDICES

CHAPTER 1

INTRODUCTION

1.1 Preface

The study of liquid-liquid extraction has become a very important subject to be discussed not just amongst chemical engineers but mathematicians as well. This type of extraction is one of the important separation technology in the process industries and is widely used in the chemical, biochemical and environmental fields. The principle of liquid-liquid extraction process is the separation of components from a homogeneous solution by using another solution which is known as a solvent [1, 2]. Normally, it is used when separation by distillation is ineffective or very difficult. This is due to the fact that certain liquids cannot withstand the high temperature of distillation.

There are many types of equipments used for the processes of liquid-liquid extraction. The concern of this research is only with the column extractor type, namely the Rotating Disc Contactor Column (RDC). Modelling the extraction processes involved in the RDC column is the major interest in this work. Modelling can be divided into two categories. One is the forward modelling and the other is the inverse modelling.

From mathematical and physical point of view, it is generally easier to calculate the "effect of a cause" or the outputs of the process than to estimate the "cause of an effect" or the input of the process. In other words, we usually know how to use mathematical and physical reasoning to describe what would be measured if conditions were well posed. This type of calculation is called a forward problem. The resulting

mathematical expressions can be used as a model and we call the process in obtaining the values of outputs as forward modelling. The concern of this research is to develop an improved mathematical model for the mass transfer process

1.2 Motivation

Several models have been developed for the modelling of RDC columns. The modelling shows that the drop size distribution and the mass transfer processes are important factors for the column performances. Since the behavior of the drop breakage and the mass transfer process involve complex interactions between relevant parameters, the need to get as close as possible to the reality of the processes is evident.

Several researchers namely Korchinsky and Azimzadih[3], Talib[4], Ghalehchian[5] and Arshad[6] had been working in this area. Korchinsky and Azimzadih[3] introduced a stage wise model for mass transfer process, which was furthered by Talib[4] and Ghalehchian[5]. The unsteady-state models developed by Talib[4] are referred to as the IAMT (Initial Approach of Mass Transfer) and BAMT (Boundary Approach of Mass Transfer). To get closer to reality, Ghalehchian[5] had developed a new steady-state model of mass transfer by including the idea of axial mixing into the simulation of the mass transfer process. Then Arshad[6] developed a new steady state model for hydrodynamic process, which updates the current hold up and drops velocities in every stage after certain time intervals until the system reaches steady state.

The mass transfer models are based on a radial diffusion equation with a constant boundary condition. However a mass transfer model with varied boundary condition has yet to be developed. The development of the model will enhance the understanding of the real process. This is because in reality the concentration of the drops in each compartment in the RDC column is not constant.

The forward model of the mass transfer process in the RDC column consists of Initial Boundary Value Problem (IBVP) of diffusion equation, a nonlinear and a few of linear algebraic equations. The details of the equations will be found in Chapter 3 to 5.

1.3 Objectives of the Research

1. To investigate an equation that will be used as the boundary condition of the IBVP.
2. To formulate a new fractional approach to equilibrium based on the IBVP of time-dependent boundary condition.
3. To formulate a modified driving force based on the new fractional approach to equilibrium.
4. To develop an algorithm for the mass transfer of a single drop in the multi-stage RDC column.
5. To develop algorithms for the mass transfer of the multiple drops in the multi-stage RDC column.

1.4 Scope of Study

This study will be based on a radial diffusion equation with varied boundary value problem for mass transfer process and a few algebraic equations governed by experiments carried out by a previous researcher for the process of hydrodynamics in the RDC column. The study will also be based on the experimental data obtained by the researchers at the University of Bradford under contract to Separation Processes Service, AEA Technology, Harwell.

1.5 Significance of the Findings

This study achieves a new development of the forward model which will provide a better simulation and hence get a better control system for the RDC column. This study also give a significant contribution in the form of algorithms. These algorithms are able to calculate the solution of the forward model for the mass transfer process in the RDC column.

1.6 Report Organization

Chapter 2 gives a literature review on liquid-liquid extraction in general. It is then followed by a review on the RDC columns including the important processes involved. The theoretical details on the drop distribution, breakage phenomena and the mass transfer process are also included. The existing forward mathematical modelling by the most recent researchers are presented. These reviews are significantly used as a background in order to develop a new mass transfer model; which will be described in Chapter 3.

Chapter 3 provides the formulation of the varied boundary function from the experimental data in [4]. The details of the exact solution of the IBVP with the time depending function boundary condition will be shown which is then followed by the derivation of the new fractional approach to equilibrium. The comparison between the new fractional approach to equilibrium and the one introduced in [7] will be made in the last section of Chapter 3.

Chapter 4 comprises the development of the forward models of the mass transfer in the multi-stage RDC column. Prior to the development, the formulation of the modified quadratic driving force which is called *Time-dependent Quadratic Driving Force(TQDF)* will be given. Based on this formulation, a Mass Transfer of A Single Drop Algorithm is designed and this is then followed by a more realistic Mass Transfer of Multiple Drops Algorithm. An alternative method for calculating the mass transfer of a Multi-Stage System will also be presented in the form of an algorithm named as the Mass Transfer Steady State Algorithm.

We then summarize the findings and suggest areas for further research in Chapter 5.

1.7 Summary

In this introductory chapter, a short introduction on the liquid-liquid extraction process particularly on the RDC column has been presented. The deficiency of the existing mass transfer models in the multi-stage RDC column has also briefly discussed.

Next, come the research objectives and scope, and the contributions of the work described in the thesis. Finally, the outline of the thesis is presented.

The current chapter serves as a defining point of the thesis. It gives direction and purpose to the research and the discussions presented here are the basis for the work done in the subsequent chapters.

CHAPTER 2

LITERATURE REVIEW

2.1 Introduction

This chapter is divided into six sections. The first section will discuss the liquid-liquid extraction and the RDC column in general. The subsequent two sections will give a brief information about the theoretical concepts and the mathematical equations used in governing the mathematical models of the processes in the RDC column. The fourth section will give a summary of the existing forward mathematical models.

2.2 Liquid-liquid Extraction

Liquid-liquid extraction is an operation that affects the transfer of a solute between two immiscible or partially immiscible liquids. The two liquids are called the feed and extraction solvent. In simple words, this is the process of the removal of the solute, say C, from the feed, say solution A, by the extraction solvent B. The solvent containing the solute C, after the extraction process is completed, is known as the extract and the solution A from which the solute C has been removed is called raffinate.

In this operation, the feed and extraction solvent, are brought into intimate contact with each other in order to extract the solute from the feed. This is actually a mass transfer operation based on the difference in concentration between two phases (the feed and the solvent) rather than the difference in physical properties.

This principle and some of the special terminology of a single contacting stage are illustrated in Figure 2.1. If equilibrium is established after contact, the stage is

defined as an ideal stage. On the laboratory scale this can be achieved in a few minutes simply by hand agitation of two liquid phases in a stoppered flask or separatory funnel [8].

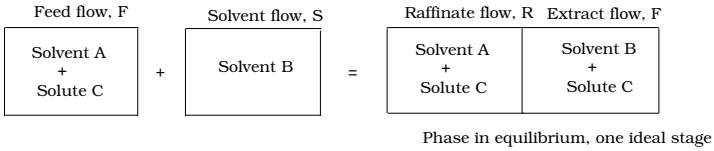

Figure 2.1: Single contacting stage

There is a wide range of applications of liquid-liquid extraction, among them are in petroleum industries, food processing, separation and purification of pharmaceutical and natural products, etc [9, 10].

Liquid-liquid extraction equipment [11, 12] can be classified as

Mixer settlers consisting of an agitated tank for mass transfer followed by a settling tank to separate both phases, due to a density difference between the two liquids. Usually it requires a series of mixer settler for a desired separation. This type of equipment is used when there will only be one equilibrium stage in the process.

Column Extractor consisting of a vertical column where the more dense phase enter at the top and flows downwards whilst the less dense phase enters at the bottom and flows upward. One of the phases can be pumped through the column at any desired flow rate, while the maximum rate of the other phase will be limited by the rate of the first phase and also the physical properties of both phases. There is a maximum rate at which the phases can flow through the column and at this rate the dispersed phase will be rejected at its point of entry and the column is said to be flooded. Thus for a particular set of process conditions, the cross sectional area of the column must be sufficiently large so that flooding does not occur. The height of the column will be set by the rate of mass transfer and the quantity of material that is required to be extracted.

There are two different types of column for the latter classification, which are non-agitated and agitated columns. For the non-agitated column such as packed and spray extraction column give differential contact, where mixing and settling proceed

continuously and simultaneously. In particular for the packed column, to make it more effective, the column is filled with packing such as Rascing or Berl saddles, which cause the droplets to coalesce at frequent intervals. For the agitated column, there is a series of disc or turbine agitators mounted on the central rotating shaft. Each agitator is separated from the next agitator by a calming section, either a mesh of wire or a stator ring, or perforated plate, that will encourage coalescence of the drops.

For the latter type of columns, such as Rotating Disc Contactor (RDC), Oldshue-Rushton Contactor, Scheibel extractor and Rotary Annular Column are widely used for liquid-liquid extraction[13]. The performance of these column contactors indicates that they are more efficient and provides better operational flexibility than non-agitated column type. In this study, we only concentrate on the RDC column. Therefore, the details of this type of column are provided in the following section.

2.2.1 Rotating Disc Contactor Column

The rotating disc contactor column is one of the agitated mechanical devices that is being widely used in the study of liquid-liquid extraction. It was initially developed in the Royal Dutch/Shell laboratories in Amsterdam by Reman in 1948-52. Some hundreds of RDCs are at present in use world-wide, ranging from less than 1m to 4.5m in diameter [14]. There is another column with 2.8 meters in diameter and 100 actual stages along the column, which is used to remove colour bodies from high molecular weight hydrocarbons (see [5]).

The mechanical layout of the RDC column is very simple and ideal for processing liquids with different densities. According to Reissinger[15] , RDCs are preferable compared to other extractor columns in the case of high through-puts and large capacity range. The RDC column consists of a vertical cylindrical column in which horizontal stator rings are installed. These rings are purposely fixed so that several compartments are formed in the column. In the middle of the compartment, flat rotating disc plates are installed, attached to a common rotating long shaft which is driven by an electric motor. The diameter of the rotor discs are smaller than the diameter of the stator opening, thus facilitating construction and maintenance. Above the top stator ring and below the bottom stator ring, settling compartments are installed. Wide -mesh

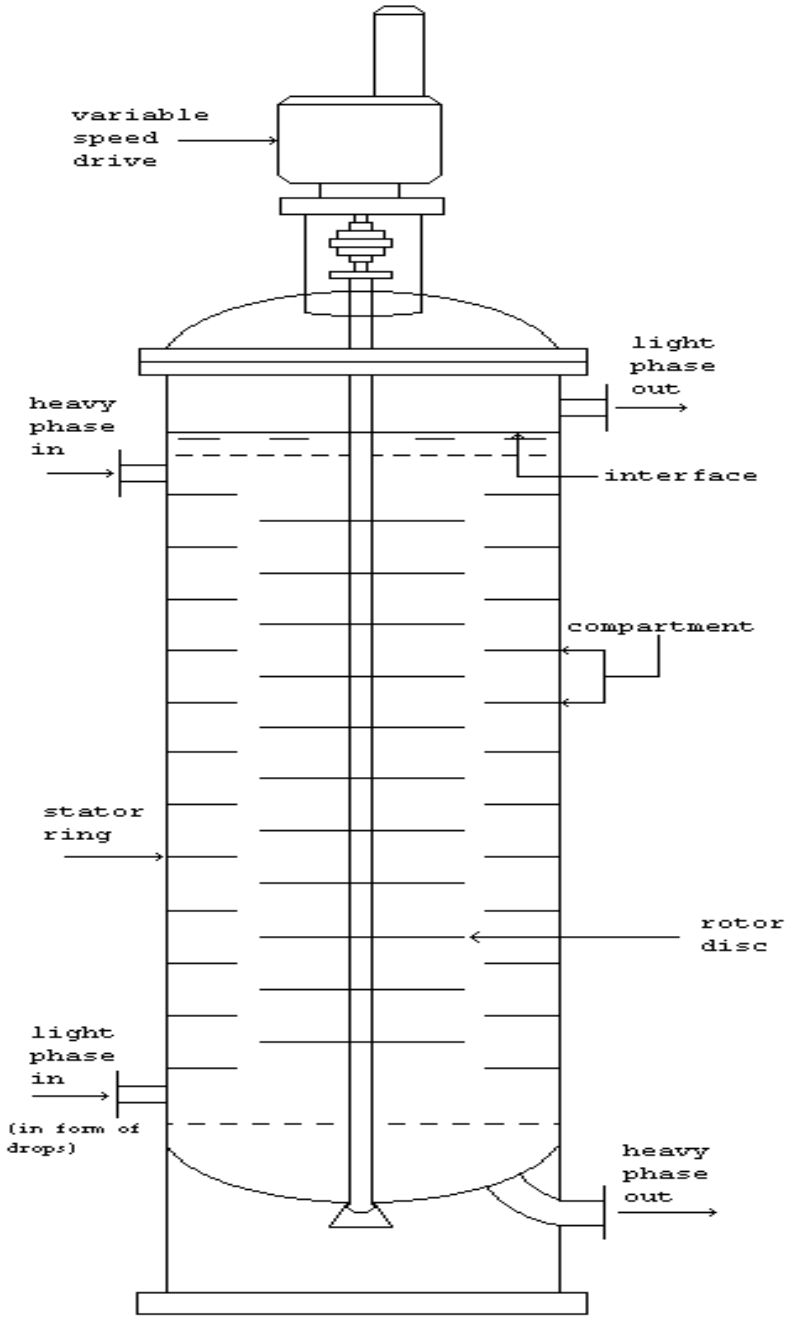

Figure 2.2: Schematic diagram of RDC column

grids are used between the agitated section and the settling zones to nullify the liquid circular motion, thus ensuring optimum settling conditions.

According to Korchinsky[16], an RDC's performance is affected by its column diameter, rotor disc diameter, stator ring opening, compartment height, number of compartments and disc rotational speed. Careful consideration must be given to these parameters in designing a satisfactory and efficient RDC column.

There are two important processes involved in the RDC column which are drop size distribution and mass transfer process [13]. Beside the parameters mentioned above, work on extraction has also shown that drop size distribution need to be determined if improvements in design are to be made. There are two factors that influence the drop size distribution which are the hydrodynamics of the drops and also the breakage process of the drops in the column. Therefore in the following section, some of the terminologies involved in the hydrodynamic process are given.

2.3 Hydrodynamics

The study of drops is more complex than that of solid particles or bubbles, because of the internal motion and the drag coefficients involved. This section begins with the review of terminal velocity of a single drop, leading to the ideas of slip velocity and characteristic velocity.

2.3.1 Terminal velocity

The terminal velocity of the drop in an infinite unhindered medium is the maximum speed of the drop motion obtained by balancing buoyancy and drag forces. The factor determining terminal velocity are drop size, drop shape and the physical properties of the system.

Based on the study of the movement of a single drop of various sizes, Grace et al. (see Talib[4]) built their own equation of terminal velocity. From these observation they found that every drop has its own terminal velocity, in which the equation involves

the dimensionless numbers i.e the Morton number, the Eotvos number and the Reynolds number. The terminal velocity equation that they proposed is

$$V_t = \left(\frac{\mu_c}{\rho_c d}\right) M^{-0.149}(J - 0.857), \tag{2.1}$$

where

$$M = \frac{g\mu_c^4 \Delta\rho}{\rho_c^2 \gamma},$$

$$J = 0.94H^{0.757} \qquad \text{for } 2 < H < 59.3,$$

$$J = 3.42H^{0.441} \qquad \text{for } H \geq 59.3,$$

$$H = \frac{4}{3} E_0 M^{-0.149} \left(\frac{\mu_c}{0.0009}\right)^{-0.14},$$

$$E_0 = \frac{gd^2 \Delta\rho}{\gamma},$$

where V_t is the drop terminal velocity, M is the Morton number, E_0 is the Eotvos number, ρ_c and μ_c are the continuous phase density and viscosity respectively, $\Delta\rho$ is the densities differences and γ is the interfacial tension.

For low values of H (i.e $H \leq 2$), terminal velocity follows the Stokes' law which is

$$V_t = \frac{g\Delta\rho d^2}{18\mu_c}. \tag{2.2}$$

2.3.2 Slip and Characteristic Velocity

Characteristic velocity is the velocity of single drop isolated from other drops but influenced by column internal, geometry and agitation.

In the 1980's many researchers made a correlation between slip velocity and other terms such as hold-up or Reynolds number according to their own experiments [17]. This led to a new development of the slip velocity and characteristic equation. Based on 117 data points Godfrey and Slater [18] obtained the characteristic velocity equation of single drop in RDC which is

$$\frac{V_k}{V_t} = 1.0 - 1.443(N_r^3 D_r^5)^{0.305} - 0.494\left(\frac{d}{D_s - D_r}\right)^{0.766}, \tag{2.3}$$

where V_k is the characteristic velocity, N_r is the rotor speed, D_r is the rotor diameter and D_s is the stator diameter.

However, according to Weiss et.al. [19], although this characteristic velocity is a function of drop diameter, it is not the actual velocity of the drops. Then in 1996 Ghalehchian[5] extended the equation to become

$$\frac{V_k}{V_t} = 1.0 - 1.443(N_r^3 D_r^5)^{0.305} - 0.494\Big(\frac{d}{D_s - D_r}\Big)^{0.766} - 4.08\frac{V_c}{V_t}. \tag{2.4}$$

The slip velocity is the relative velocity of drops with respect to the continuous phase. Under counter current flow as in RDC, the slip velocity is given by

$$V_s = \frac{V_d}{X} + \frac{V_c}{1 - X}. \tag{2.5}$$

Godfrey and Slater [18] showed that the slip velocity can also be represented as a function of characteristic velocity and hold-up, X, that is

$$V_s = V_k(1 - X)^m, \tag{2.6}$$

where V_k is the characteristic velocity, $m = 0.129\sqrt{Re_k}$ and $Re_k = \frac{\rho_c V_k d_i}{m u_c}$.

Applying the equation of slip velocity for each drop fraction, with assumption that the amount of hold-up is uniform around all drop fractions, the basic hydrodynamic equation may be written as

$$V_d = V_k(1 - X)^m - \frac{V_c X}{1 - X}. \tag{2.7}$$

2.4 Drop Breakage Phenomena

In an RDC column, the drops are dispersed into the column through a distributor. This distributor is located at the bottom of the column. These drops will rise up the column and will break into smaller drops of different sizes as they hit the rotating discs. In the following subsections the important terms of the drop breakage phenomena are given in order to understand the factors that affect the breakage of drops in the column.

2.4.1 Drop Size

Drop size is a very important variable affecting the hydrodynamic and mass transfer processes. Several researchers studied the drop breakage in liquid-liquid system in the RDC column [20, 21, 22, 16]. From these studies, they concluded that Weber and Reynolds numbers are required to correlate the parameters involves for the drop breakage factors in the column. According to Korchinsky [16], the smaller drop required larger column diameter, because of lower slip velocities relative to the continuous phase but provide larger specific interfacial surface area.

Knowledge on the prediction of column drop size is an important factor in performance prediction or designing of RDC column. Large number of relatively stationary small drops will decrease the column capacity. Larger drops will have larger volume, low surface area per unit volume, higher slip velocity which means that the column height must be increased to effect satisfactory extraction efficiencies for such drops.

2.4.2 Maximum Drop Size

In a dispersion process there is a maximum drop diameter above which no drop can exist in a stable condition. Kolmogrov's theory of local isotropic turbulence was used by Hinze [23] in 1955 to describe this maximum drop size. There is a relationship between the power consumption per unit mass and the power consumption per disc in a compartment with the later depending on disc Reynold number. Later more work were done by Strand et al. [24], Zhang et al. [25], Slater et al. [26] and Chang-Kakoti et al. [27]. Using several sets of data from different sources, Chang-Kakoti et al. [27] found a correlation between the maximum drop size and the Sauter mean drop size, to be

$$d_{max} = 2.4 d_{32}^{0.8}, \tag{2.8}$$

where

$$d_{32} = 3.6 \times 10^{-5} \left(\frac{h_c}{D_r}\right)^{0.18} P^{0.13} E^{0.21}. \tag{2.9}$$

$P = \frac{\rho_c^2 \gamma^3}{g \mu_c^4 \Delta\rho}$, $E = \frac{4P_R}{\pi d_c^2 h_c \rho_c}$ and

$P_R = 6.87 \times Re_D^{-0.658} \rho_c N_r^3 D_r^5 \qquad Re_D < 6 \times 10^4$

$P_R = 0.069 \times Re_D^{-0.155} \rho_c N_r^3 D_r^5 \qquad Re_D \geq 6 \times 10^4$

2.4.3 Drop Breakage

Drop breakage in liquid-liquid system is induced by the effect of high shear stress or by the influence of turbulent inertial stress. However as the diameter of the drop decreases, the deforming stress across it also decreases. Due to these phenomena a diameter is finally reached where the deforming stress is unable to break the drop.

2.4.4 Critical Drop Size and Critical Rotor Speed

Critical drop size is the maximum drop size below which drop do not break for a given rotor speed. Correspondingly, for a given drop size in the column, the minimum rotor speed below which no drop will break is called the critical rotor speed. This rotor speed was given by Cauwenberg et al. [28],

$$N_{cr} = 0.802 \frac{\gamma^{0.7}}{\rho_c^{0.3} \mu_c^{0.4} d_i^{0.59} D_r^{0.71}} \tag{2.10}$$

for both laminar and turbulent regions. According to him, this relationship has shown good agreement with the experimental data in RDC columns of different sizes $(152, 300, 600mm)$. He also found that the equation of critical drop size is

$$d_{cr} = 0.685 We_{D,\omega}^{-1.2} Re_{D,\omega}^{0.7} D_r, \tag{2.11}$$

where the disc angular Weber number and the Reynolds number are of the forms

$$We_{D,\omega} = \frac{\rho_c (2\pi N_r)^2 D_r^3}{\gamma}, \tag{2.12}$$

and

$$Re_{D,\omega} = \frac{\rho_c 2\pi N_r D_r^2}{\mu_c}, \tag{2.13}$$

respectively.

2.4.5 Initial Number of Drops

The initial number of drops in an RDC could be controlled by the distributor but basically it depends on the flow rate of dispersed phase, F_d and the size of initial drop [6], that is

$$\frac{Number \quad of \quad drops}{unit \quad time} = \frac{3F_d(d_0/2)^{-3}}{4\pi}. \tag{2.14}$$

These drops are dispersed through the distributor, which is located at the top or bottom of the column. The counter current flow of the phases can be achieved by introducing different densities of liquid. The drops will rise up the column if their density is less than that of the continuous phase. When the drops move through the medium in the column, they will hit the rotating discs and will possibly break into smaller drops until they arrive at the settling compartment.

2.4.6 Probability of Breakage

The probability of breakage for a given drop size is defined as the ratio of number of broken drops and the total number of drops observed in a large sample number. In 1991, Bahmanyar and Slater [21] had introduced this idea of breakage probability. Based on this idea, Cauwenberg et al. [28] had developed an equation of breakage probability, P, for laminar region ($Re_{D,\omega} < 10^5$) and turbulent region ($Re_{D,\omega} > 10^5$) which are

$$P = \frac{0.258We_{D,\omega,m}^{1.16}}{1 + 0.258We_{D,\omega,m}^{1.16}}, \tag{2.15}$$

and

$$P = \frac{0.00312We_{D,\omega,m}^{1.01}}{1 + 0.00312We_{D,\omega,m}^{1.16}}, \tag{2.16}$$

where $We_{D,\omega,m}$ represents as a modified Weber number that is

$$We_{D,\omega,m} = \frac{\rho_c^{0.5}\mu_c^{0.5}(\omega^{1.5} - \omega_{cr}^{1.5})D_r d_i}{\gamma}, \tag{2.17}$$

and

$$We_{D,\omega,m} = \frac{\rho_c^{0.8}\mu_c^{0.2}(\omega^{1.8} - \omega_{cr}^{1.8})D_r^{1.6}d_i}{\gamma}, \tag{2.18}$$

respectively.

2.4.7 Mean Number of Daughter Drops Produced

The breakage of a drop will result in various numbers and sizes of daughter drops. The number of daughter drops produced depends on the initial mother drop size, physical properties and agitation speed. Many researches have been carried out by previous researchers concerning the mean number of daughter drops produced. Starting from Hancil and Rod in 1981, followed by Eid (see [6]) then finally Bahmanyar and Slater [21] worked out experiments using different chemical systems. The data obtained were well represented by the equation

$$X_m = 2 + 0.9\big(\frac{d_i}{d_{cr}} - 1\big), \tag{2.19}$$

where d_i is mother drop size, X_m is number of daughter drops produced and d_{cr} is the critical drop size at the appropriate agitation speed.

Also, from the work done by Coulaloglou and Tavlarides [29] and Jares and Prochazka [30] concerning the the drop distribution of daughter drops produced, they found that the Beta distribution function fits the experimental data in most column including RDC. The Beta probability density function which is related to this distribution can be written in the form

$$f(X_m, y) = (X_m - 1)(1 - y)^{X_m - 2} \tag{2.20}$$

y is volume ratio of daughter drops to mother drops ie d_d^3/d_m^3.

2.5 Mass Transfer

In a single phase system, the mass transfer is defined as the movement of mass or molecules from an area of high concentration to that of low concentration until a homogeneous or equilibrium concentration in the system is achieved. Basically, there are two modes of mass transfer in a single liquid phase:

Molecular Diffusion This type of diffusion occurs in the absence of any bulk motion of the liquid. In this mode, the phase will tend to a uniform concentration as a result of the random motion of the molecules.

Eddy Diffusion Meanwhile eddy diffusion occurs in turbulent flow processes because of the existence of bulk motion of the molecules. The phase will tend to a uniform concentration due to agitation.

The mass transfer process in the RDC column considered in this study involves liquids in turbulent flow. In this column, mass transfer will occur whenever there is a concentration gradient between the two phases in direction of decreasing concentration. The rate of mass transfer of materials from one phase to the other depends on the mass transfer coefficient. The prediction of mass transfer coefficient have been studied by many researchers and recently by Slater et al.[26] and Bahmanyar et al.[31] on mass transfer rates of single drop in short RDCs and non-flowing continuous phase. In the following subsection we provide some theories associated with mass transfer before the modelling of mass transfer in the RDC column is discussed.

2.5.1 The Whitman Two-film Theory

This theory is the earliest and simplest theory of mass transfer between two liquids phases across a plane interface [32] . It assumes that there is a thin layer on both sides of the interface. In this thin film, resistance to mass transfer exists. The mass transfer across these films is assumed to take place by molecular diffusion. Outside these films the bulk concentration of the liquid phases are uniform which is brought about by the eddy diffusion. The eddy diffusion caused by the turbulence in the bulk is considered to vanish abruptly at the interface of the films. It is assumed that equilibrium is established between the two phases at the interfaces. Therefore any resistance to transfer at the phase boundary is non-existent.

In order to describe the above process explicitly, let two liquids X and Y with bulk concentrations, x_b and y_b respectively where the direction of mass transfer is assumed from the X phase to the Y phase. The schematic diagram in Figure 2.3 will describe the process. In the X phase, mass transfer at a steady state from the bulk

concentration to the interface is described by the equation

$$J_x = k_x(x_b - x_i), \tag{2.21}$$

and for the Y phase, the mass transfer is from the interface to the bulk concentration which is

$$J_y = k_y(y_i - y_b), \tag{2.22}$$

where J_x and J_y are known as *flux* or rate of mass transfer. Meanwhile k_x and k_y are the mass transfer coefficients for the liquids X and Y respectively.

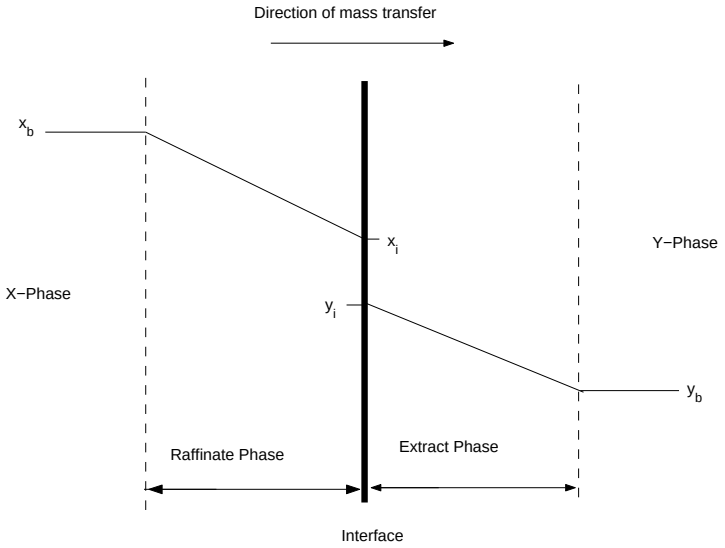

Figure 2.3: Mass transfer at interface

Since equilibrium is established between the two phases at the interface, the fluxes must be the same. Thus

$$k_x(x_b - x_i) = k_y(y_i - y_b). \tag{2.23}$$

The expression governing the equilibrium at the interface is known as equilibrium relation or equation. For example, the equilibrium relation for cumene-isobutyric acid-water system is derived from the distribution of isobutyric acid (the solute) between cumene and water data reported by Bailes et al. [33]. From this data the equilibrium equation for the system is obtained which is

$$C_d = 0.135C_c^{1.85}, \tag{2.24}$$

where C_d and C_c are concentrations of isobutyric acid in cumene and aqueous respectively. Another example is the equilibrium equation of butanol-succinic acid-water system where the equation is

$$C_d = 1.086C_c - 0.849 \times 10^{-3}C_c^2 - 0.162 \times 10^{-4}C_c^3. \tag{2.25}$$

2.5.2 The Penetration Theory

In Whitman two-film theory, we only consider the mass transfer across the interface as a steady-state process of molecular diffusion whereby in this study the process of mass transfer in RDC column is actually an unsteady-state process. Therefore a theory proposed by Higbie (see Slater[34]) known as penetration theory is introduced here.

The theory was about a mechanism of mass transfer involving the following processes:

- The movement of eddies from the bulk of a fluid with concentration c_b to the interface at a distance z from its original position.
- At the interface the solute transfer takes place by unsteady state molecular diffusion for a short exposure time t.
- This bulk of fluids is then being replaced by another bulk of fluids as a result of eddy diffusion.

The equation governing the transfer process is given by

$$\frac{\partial c}{\partial t} = D\frac{\partial^2 c}{\partial z^2} \tag{2.26}$$

with the initial and boundary conditions

$$c = c_b, \quad z > 0, \quad t = 0 \tag{2.27}$$

$$c = c_i, \quad z = 0, \quad t > 0 \tag{2.28}$$

$$c = c_b, \quad z \to \infty, \quad t > 0 \tag{2.29}$$

The solution of the above diffusion can be shown as

$$c - c_b = (c_i - c_b)(1 - \frac{2}{\sqrt{\pi}} \int_0^{\frac{z}{\sqrt{4Dt}}} exp(-u^2)du), \tag{2.30}$$

where $\frac{2}{\sqrt{\pi}} \int_0^{\frac{z}{\sqrt{4Dt}}} exp(-u^2)du$ is readily evaluated since it is actually a tabulated error of function ($\text{erf}(\frac{z}{\sqrt{4Dt}})$). Therefore the expression (2.30) can be written as

$$c - c_b = (c_i - c_b)(1 - erf(\frac{z}{\sqrt{4Dt}})). \tag{2.31}$$

By Fick's first law [34], the rate of mass transfer per unit area across the interface at any instant can be found by evaluating

$$\begin{aligned} J_t &= -D \left(\frac{\partial c}{\partial t} \right)_{z=0} \\ &= (c_i - c_b)\sqrt{\frac{D}{\pi t}}. \end{aligned} \tag{2.32}$$

Averaging over time of exposure, t_e, gives

$$\begin{aligned} J &= \frac{(c_i - c_b)}{t_e} \int_0^{t_e} \sqrt{\frac{D}{\pi t}}\, dt \\ &= 2(c_i - c_b)\sqrt{\frac{D}{\pi_e}}. \end{aligned} \tag{2.33}$$

From (2.22) and (2.23), the film mass transfer coefficient of the continuous and dispersed phase are $k_x = 2\sqrt{\frac{D}{\pi_e}}$ and $k_y = 2\sqrt{\frac{D}{\pi_e}}$ respectively.

2.5.3 Dispersed Phase Mass Transfer Coefficient

Several theoretical models have been proposed for the estimation of the dispersed phase mass transfer coefficient (Godfrey and Slater[18]). They found that the dispersed phase mass transfer coefficient, k_d is time-dependent. In general, three situations arise depending on the state of the drops which are

- Molecular diffusion − Newman developed an equation for resistance in a solid sphere that is

$$k_d = -\frac{d}{6t} ln\big[\frac{6}{\pi^2} \sum_1^{\infty} \frac{1}{n^2} exp \frac{-4n^2\pi^2 D_d t}{d^2}\big]$$

Then, in 1953, Vermeulen[35] proposed a useful approximation to this equation as in Talib[4], ie

$$k_d \approx -\frac{d}{6t} ln\big[1 - (1 - exp\frac{-4n^2\pi^2 D_d t}{d^2})^{1/2}\big]$$

- Circulating of drop − A circulating motion inside drops is induced by drag forces arising from relative velocity of motion between a drop and continuous phase. Kroglg and Brink (see [6]) provided a general solution for the problem of heat transfer which can be used for both phases . Then this idea was expanded by Calderbank and Korchincki to obtain an equation for the mass transfer coefficient in drops with laminar internal circulation (see Godfrey and Slater[18]). The equation is

$$k_d = -\sqrt{2.25}\frac{d}{6t} ln\big[\frac{6}{\pi^2}\sum_{1}^{\infty}\frac{1}{n^2} exp\frac{-4n^2\pi^2 D_d t}{d^2}\big]$$

- Oscillating drops − As drops become larger their shape may change due to the nature of drag force involved. At some critical size, drops can start to oscillate in shape and drag force are such that terminal velocity decrease as the drop size increase further. Many models have been proposed to predict mass transfer coefficient under oscillating condition. Skelland et al. [36] suggested that

$$k_d = 31.4\frac{D_d}{d}\big(\frac{4D_d t}{d^2}\big)^{-0.43}\big(\frac{\mu_d}{\rho D_d d}\big)^{-0.125}\big(\frac{V^2\rho_c}{\gamma}\big)^{0.37}.$$

2.5.4 Continuous Phase Mass Transfer Coefficient

There are three types of flow around the drops which influence the transfer of solute from outside a stagnant drop. They are radial diffusion, natural convection and forced convection. The continuous phase mass transfer coefficient for these types of flow are correlated as a Sherwood number and are given respectively as

$$Sh_c = a_1$$

where a_1 is a constant,

$$Sh_c = a_1 + a_2\big(\frac{g\rho_c\Delta\rho d^3}{\mu_c^2} Sc_c\big)^n,$$

where Sc_c is Schmidt number defined as $Sc_c = \mu_c\rho_c D_c$, a_1, a_2, n are constants and $\Delta\rho$ is the difference in density and

$$Sh_c = a_1 + a_2(Rf)^n(Sc_c)^l,$$

where a_1, a_2, n, l are constants.

The transfer is by radial diffusion if the continuous phase is stagnant. Whilst the transfer is by natural convection if the continuous phase around the drop is subjected to convection. For the latter type of flow, the transfer is by forced convection if the continuous phase around the drop is subject to an external force forcing the continuous phase to flow past the drop with velocities up to those of complete turbulence.

2.5.5 Overall Mass Transfer Coefficient

If the equilibrium distribution of solute strongly favours one phase, then the principle resistance to mass transfer lies in the other phase. A brief explanation about this concept can be found in [6]. In this work, the required overall dispersed phase mass transfer coefficient, K_{od_i} for drops with size d_i in stage n, is defined as

$$K_{od_i} = \frac{d_i}{6t_i} ln\big(\sum_{n=1}^{\infty} \frac{6L^2}{\beta_n^2(\beta_n^2 + L(L-1))} exp\big(- \frac{4D_d \beta_n^2 t_{r,i}}{d_i^2}\big)\big),$$

where, L known as Sherwood number, $\beta_n \cot \beta_n + L - 1 = 0$. The first six values of β_n for specified value of L are given by Crank[7].

2.6 The Existing Forward Mathematical Models of the Processes in the RDC column

In this section, the existing forward mathematical model of the processes involved in the RDC column are reviewed. This review only covers the most recent researches on the models which were produced by Talib[4], Ghalehchian[5] and Arshad[6] and Mohamed[37].

2.6.1 Talib's work

Drop Distribution Model (Hydrodynamic Model)

Talib had modelled the break-up process for the drops moving up the RDC column by assuming that each compartment has ten numbers of classes or cells of equal widths which hold drops with sizes in the specified range.

Light phase drops entering the extraction column from the distributer has the chance of breaking into smaller drops on hitting the first rotor disc. The drops then moved into the first compartment. Depending on their sizes, the drops are placed in the appropriate cell. In a given cell all drops are then treated as having the same average diameter size when considering possible breakage as they moved past the next disc. Continuing in this way up the column, the number of drops and their size distribution for all the compartments in the column can be determined.

In Talib's work, the distribution of the drops were determined by two methods namely the Monte Carlo and the Expected Value methods. In the simulation drop break-up using the Monte Carlo Method, drops are considered as entering and moving up the column one at a time. Meanwhile, the simulation by the latter method considered the break-up of a swarm of N drops. Beside that, the simulation of drop break-up using this method uses the probability, p and beta distribution, $\phi(x, y)$ differently from the first method which uses random number.

Even though the distribution of the drops are found to be similar for both methods, Talib concluded that the latter method was more efficient due to the less simulation time needed and data requirement. The Monte Carlo Method requires detailed information including the number of daughter drops produced from the break-up of a drop, which depends on the size of the mother drop, the rotor speed and the liquid used. However, the Expected Value Method requires only the average number daughters produced.

Furthermore, Talib had introduced another model, Dynamic Expected Value Method which was a modification of the EVM. The model was expected to give a more realistic representation because it is based on different drop velocities for each class of the drops whilst in the previous model, it was assumed that all drops have the same velocity irrespective of their sizes.

Mass Transfer Model

In Talib's early work, he had introduced two unsteady stage-wise models of the mass transfer process in the RDC column namely the Initial Approach of mass Transfer(IAMT) and the Boundary Approach of mass Transfer (BAMT). The first model is based on the start up process of the drops entering a column with an

undisturbed continuous phase whilst the second model is based on the presence of drops throughout the length of the RDC column.

Talib also introduced the concept of the diffusion in a sphere, the theory of the film mass transfer coefficients and the two film-theory. Beside that at the early development of the models, Talib used the linear driving force for both the drop and the continuous phases. Since the interface of a liquid drop in a continuous phase is spherical in RDC column, Vermuelen[35] stated that the driving force in a drop can be considered as non-linear which is known as the quadratic driving force. Talib then incorporated this idea into the IAMT mass transfer model.

2.6.2 Ghalehchian's work

In Ghalehchian's work, hydrodynamic and mass transfer experimental results from a pilot RDC column of 23 stages were used. Then a new stage wise model with back-flow was developed. The model took into account the influence of drop breakage at each stage.

Generally, Ghalehchian had produced the new steady state model of mass transfer which is also basically based on the mathematical equation discussed in Talib[4]. Figure shows the stage wise mass transfer process, where e is the back-flow coefficient which is equal to F_d/F_c. F_d and F_c here, are dispersed and continuous phase flow rate. The new model was said to be more realistic by including the idea of axial mixing. The model also considered the extraction of unclean solution.

2.6.3 Mohamed's work

In Mohamed's work, the mathematical modelling of simultaneous drop diffusing in RDC column is developed. In this model, it is assumed that the distribution of the drops in the column is in equilibrium and the mass transfer from the continuous phase to every drop occur simultaneously.

The total concentration for every drop is obtained by the Simultaneous Discrete Mass Transfer(S-DMT) model. The model is actually based on Discrete Mass Transfer

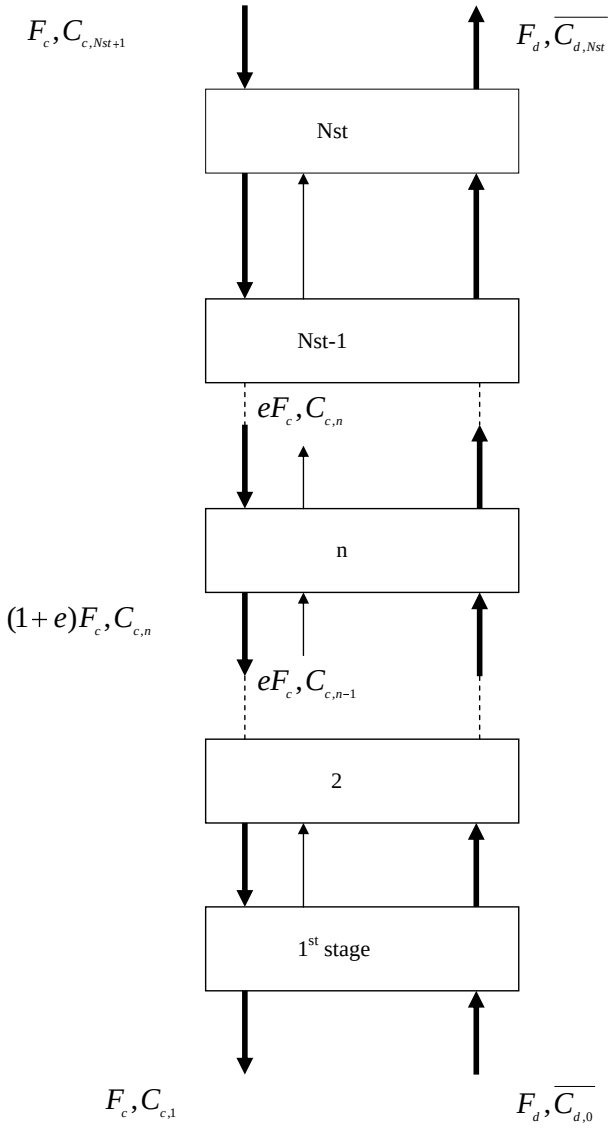

Figure 2.4: Stage wise back-flow for mass transfer process

Model as discussed in Talib[4]. From the model, Mohamed concludes that the two drops will provide more cross-section area for the mass transfer compared to a drop for same total volume.

2.6.4 Arshad's work

In Arshad's work, the hydrodynamic model is close to reality by following the process from an undisturbed state into steady state. The model was found to reach steady state quicker compared with Talib's. The model was expected to update the

value of the hold-up and the velocities of the drops moving up the column before they reach the final stage. Then Arshad used the mass transfer model developed by Ghalehchian to combine with the new hydrodynamic model. Arshad considered four different physical/chemical systems of two different sizes of the RDC column.

In addition, Arshad observed and analyzed the simulation data to examine the effects of varying input variables on output values yield. The analysis was done by Principle Component Analysis (PCA) method. Arshad also had provided a review on Artificial Neural Network (ANN) and Fuzzy Logic (FL) modelling. At the final stage of his work, Arshad had introduced these concept to the RDC system.

2.7 Summary

In the beginning of this chapter, an overview of liquid-liquid extraction process was provided. A review has been given, starting with the principle of the process and it was then followed by the classification of the extraction equipment. To achieve the aim of this research, the review on the RDC column was briefly given including the important processes involved.

The mass transfer in the column are effected by the drop distribution and breakage phenomena. The detailed description about these terms were provided leading to the review on the mass transfer itself. The theoretical details on the mass transfer coefficient were also included. A review on existing forward mathematical modelling by the most recent researchers were also presented. These reviews are significantly used as a background in developing a new mass transfer model; the works are detailed starting in Chapter 3.

CHAPTER 3

THE FORWARD MASS TRANSFER MODEL

3.1 Introduction

The existing mass transfer models mentioned in Chapter 2 were based on a radial diffusion equation with constant boundary conditions. However a mass transfer model with varied boundary conditions has yet to be developed. Therefore, in this chapter, a modified forward mass transfer model with time dependent function boundary condition will be discussed. This function is derived from the experimental data obtained in [4].

Following this derivation, Section 3.3.1 presents the details on how the solution of the diffusion equation of the time varying boundary condition is obtained. This is followed by the derivation of the *new fractional approach to equilibrium*. In Section 3.4, the simulations for different drop sizes are carried out to see their effects on the new fractional approach to equilibrium. Then a comparison between the fractional approach to equilibrium introduced in [7] and the new one is also carried out in the last section of this chapter.

3.2 The Forward Mass Transfer Model

In the RDC column, the mechanism of mass transfer across an interface between two liquid phases is based on penetration theory. This theory was proposed by Higbie in 1935 (see Slater [34]), which assumed that a packet of fluid with bulk concentration travel to the interface at a distance from its original position. At the interface, the fluid

packets undergo molecular diffusion for a short exposure of time, before being replaced by another fluid packet.

The model discussed in this chapter is based on the model of the mass transfer developed by Talib [4]. Talib [4] assumed that at each stage i, the drop has an initial uniform concentration as well as the concentration of the medium phase. When a drop enters a stage i, solutes from the uniform medium concentration surrounding the drop are transferred to the drop or vice versa depending on the concentration difference between the drop and the medium. In this study, only the transfer of solute from the medium to the drop will be considered.

The study of the shape of the moving drops has been found useful in understanding the dynamics of the moving drops since the drag on the drops depends on their shapes during movement in another medium. The shape of liquid drops moving in liquids is dependent on the balance between the hydrodynamic pressure exerted on account of the relative velocities of the drop and field liquids, and the surface forces which tend to make the drop a sphere. In this study we assume that all the drops are spherical in shape, therefore the amount of solute transferred to the drops can be obtained by using the concept of diffusion in a sphere.

3.2.1 Diffusion in a Sphere

Consider a sphere of radius a. The radial diffusion equation is

$$\frac{\partial C}{\partial t} = D\left(\frac{\partial^2 C}{\partial r^2} + \frac{2}{r}\frac{\partial C}{\partial r}\right) \tag{3.1}$$

where $C = C(r,t)$ is the concentration at distance r from the center of the sphere at time t and D is the diffusion constant.

If we make the substitution $u = Cr$, Equation (3.1) becomes

$$\frac{\partial u}{\partial t} = D\frac{\partial^2 u}{\partial r^2} \tag{3.2}$$

If the sphere of radius a has initial uniform concentration c_1 and the surface of the sphere is maintained at a constant concentration c_0, the diffusion equation of the sphere with a constant diffusion coefficient D is given by the initial boundary value problem (IBVP),

$$\begin{aligned} \frac{\partial u}{\partial t} &= D\frac{\partial^2 u}{\partial r^2}, \quad 0 \le r < a, \quad t \ge 0 && (3.3)\\ u(0,t) &= 0, \quad t > 0 && (3.4)\\ u(a,t) &= ac_0, \quad t > 0 && (3.5)\\ u(r,0) &= rc_1, \quad 0 \le r < a && (3.6) \end{aligned}$$

These equations can be solved by the method of separation of variables.

Setting $u(r,t) = R(r)T(t)$, we will get an ordinary differential equation of

$$\frac{R''}{R} = \frac{T'}{DT} = -\lambda^2,$$

where λ^2 is a separation constant. Thus the general solutions for the space and time variations are given as below,

$$\begin{aligned} R(r) &= \begin{cases} B_1 + B_2 r, & \lambda = 0 \\ A_1 \cos\lambda r + A_2 \sin\lambda r, & \lambda \neq 0 \end{cases} \\ T(t) &= \begin{cases} B_3, & \lambda = 0 \\ Be^{-D\lambda^2 t}, & \lambda \neq 0 \end{cases} \end{aligned} \qquad (3.8)$$

Therefore, the general solution for $u(r,t)$ is

$$u(r,t) = R(r)T(t) = \begin{cases} (B_1 + B_2 r)B_3, & \lambda = 0 \\ (A_1 \cos\lambda r + A_2 \sin\lambda r)Be^{-D\lambda^2 t}, & \lambda \neq 0 \end{cases}$$

where $A_1, A_2, A_3, B, B_1, B_2, B_3$ are the arbitrary constants.

Simplifying the above equation, we get

$$u(r,t) = \begin{cases} (H + Ir), & \lambda = 0 \\ (J \cos\lambda r + K \sin\lambda r)e^{-D\lambda^2 t}, & \lambda \neq 0 \end{cases}$$

Using the superposition rule, we get

$$u(r,t) = (H + Ir) + (J \cos\lambda r + K \sin\lambda r)e^{-D\lambda^2 t},$$

subject to boundary condition of Equations (3.4) and (3.5), we get

$$u(0,t) = 0 = H + Je^{-D\lambda^2 t}, \qquad t > 0 \tag{3.12}$$

Since the coefficient of H and $e^{-D\lambda^2 t}$ are linearly independent on the t interval, it follows from (3.12) that we need $H = 0$ and $J = 0$, thus

$$u(r,t) = Ir + K \sin \lambda r e^{-D\lambda^2 t},$$

and

$$u(a,t) = ac_0 = Ia + K \sin \lambda a e^{-D\lambda^2 t}, \qquad t > 0$$

or

$$a(c_0 - I) - K \sin \lambda a e^{-D\lambda^2 t} = 0. \qquad t > 0 \tag{3.15}$$

Again invoking the linear independence of coefficient of $a(c_0 - I)$ and $e^{-D\lambda^2 t}$, it follows from (3.15) that $a(c_0 - I) = 0$ and $K \sin \lambda a = 0$, which gives

$$\begin{aligned} I &= c_0 \\ K &= 0, \quad \text{or} \quad \sin \lambda a = 0, \quad \text{(or both)} \end{aligned}$$

Here, the rule is to make the choice so as to maintain as robust a solution as possible, then we take $\sin \lambda a = 0$ implies $\lambda_n = \frac{n\pi}{a}$ for $n = 1, 2, 3, ...$

Thus the solution becomes

$$u(r,t) = c_0 r + \sum_{n=1}^{\infty} K_n \sin \frac{n\pi r}{a} e^{\frac{-Dn^2\pi^2 t}{a^2}}.$$

To find the K_n, and hence to complete the solution of the problem, we now set $t = 0$ in the expression on the right and replace $u(r,0)$ by the initial condition $u(r,0) = rc_1$, then we obtain

$$u(r,0) = rc_1 = c_0 r + \sum_{n=1}^{\infty} K_n \sin \frac{n\pi r}{a},$$

or

$$r(c_1 - c_0) = \sum_{n=1}^{\infty} K_n \sin \frac{n\pi r}{a}.$$

This shows that the K_n are the coefficients in the half-range Fourier sine series expansion of $r(c_1 - c_0)$ over the interval $0 \le r \le a$. Thus the K_n are given by

$$K_n = \frac{2}{a} \int_0^a r(c_1 - c_0) \sin \frac{n\pi r}{a} dr,$$

and so

$$K_n = \frac{-2a}{n\pi}(c_1 - c_0)(-1)^n.$$

Thus the solution of IBVP of (3.3)-(3.6) becomes

$$u(r,t) = c_0 r + \frac{2a}{\pi}(c_0 - c_1)\sum_{n=1}^{\infty}\frac{(-1)^n}{n}\sin\frac{n\pi r}{a}e^{\frac{-Dn^2\pi^2 t}{a^2}} \tag{3.21}$$

or

$$C(r,t) = c_0 + \frac{2a}{\pi r}(c_0 - c_1)\sum_{n=1}^{\infty}\frac{(-1)^n}{n}\sin\frac{n\pi r}{a}e^{\frac{-Dn^2\pi^2 t}{a^2}}, \tag{3.22}$$

where $C(r,t)$ is the concentration of the drop at time t. In our work, we are interested in the average concentration of the sphere, C_{av}, given by equation

$$C_{av} = \frac{C_t}{4\pi a^3/3}, \tag{3.23}$$

where the total concentration C_t of the sphere is obtained from

$$C_t = \int_0^a C(r,t)4\pi r^2\, dr. \tag{3.24}$$

According to Crank [7], the total amount of diffusing substance entering or leaving the drop which is denoted as *fractional approach to equilibrium* is used to relate the analytical results to a mass transfer coefficient that is

$$F = \frac{C_{av} - c_1}{c_0 - c_1} \tag{3.25}$$

where C_{av} is the average concentration of the drop at time t and c_1 and c_0 are the initial and boundary concentrations respectively.

Using this concept, the fractional approach to equilibrium is derived for the problem of equations (3.3) to (3.6) , which is

$$F_c(t) = 1 - \frac{6}{\pi^2}\sum_{1}^{\infty}\frac{1}{n^2}(e^{\frac{Dn^2\pi^2 t}{a^2}}), \tag{3.26}$$

where the subscript c in F_c indicates that this term is already derived by Crank [7].

3.3 The Modified Model

As mentioned in previous section, we are interested in developing an improved model of mass transfer of which the boundary condition is a function of time. To

achieve this, we consider the normalized data obtained from the experimental work of mass transfer in the RDC column with $152mm$ diameter and 23 stages of the iso-butyric acid/cumene/watersystem (Talib [4]). In this system the iso-butyric acid in water is acting as the feed(continuous phase) and the cumene is the solvent(dispersed phase). The geometrical details of the RDC column used and the physical properties of this system are given in Appendices A.1 and A.2.

Table 3.1: Normalized dispersed and continuous phase concentrations

Stage number	dispersed(drop)	continuous(medium)
0	0	0.912
7	0.118	0.947
11	0.162	0.960
15	0.232	0.981
19	0.269	0.992
23	0.285	0.997
24	0.294	1.00

Note: Stage 0 in Table 3.1 is the feed and exit for the dispersed and continuous phases respectively and stage 24 is the exit and feed for the dispersed and continuous phases respectively.

From the normalized data (see Table 3.1), we find that the concentration of the continuous phase depends on the stage of the RDC column (the concentration is lesser at the lower stage than the upper stage). This phenomenon has shown that there is a mass transfer from the continuous to the dispersed phase. To relate the changes of concentration with time, we consider 10 different classes of drops being formed from a single mother drop as the mother drop hits the first rotor disc of the column. These 10 different sizes of daughter drops have different velocities depending on their sizes. The velocity of the drops can be calculated using equation

$$v = v_k(1-h)^m, \tag{3.27}$$

where v_k is the characteristic velocity of the drop. h is the hold up which is defined as the ratio of the total volume of the freely moving drops present in the column to the

volume of the column and m is a constant.

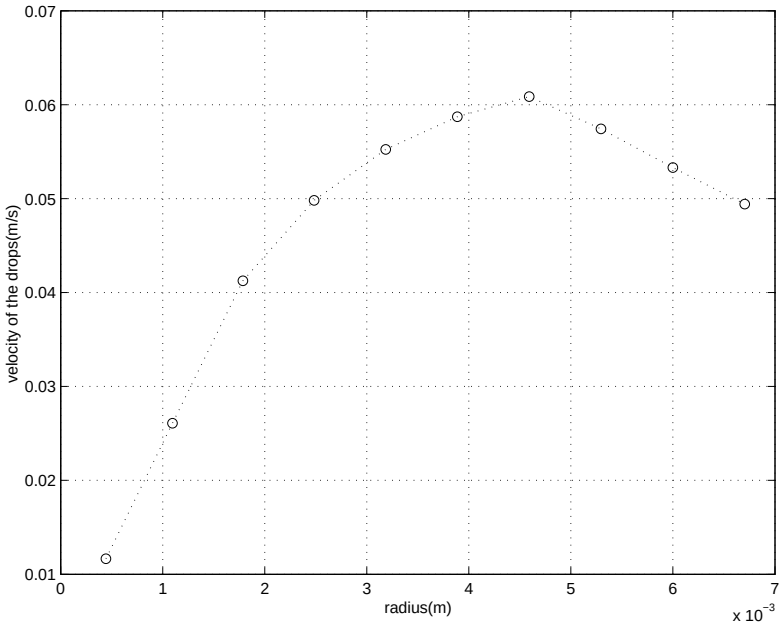

Figure 3.1: The velocity of 10 different sizes of drops in the RDC column.

The velocity of each drop is plotted against time as in Figure 3.1. From these velocities the time spent by each drop in the compartment can be found. The residence time for each size of the drop is tabulated in Table 3.2. The relationship between the concentration of the continuous phase and the time taken for the 10 different sizes of drops to reach a particular stage of the column can then be established. To achieve this, we use the least squares method. In this method, we have to predict the relationship between the two parameters by letting $\hat{f}_1$ as the predicted function of the concentration of the continuous phase where $\hat{f}_1 = \hat{a_{1i}} + \hat{b_{1i}}t$ by a given value of t. The values of $\hat{a_{1i}}$ and $\hat{b_{1i}}$ can be obtained from

$$\hat{b_{1i}} = \frac{S_{i_{t_i f_1}}}{S_{i_{t_i t_i}}}$$

and

$$\hat{a_{1i}} = \bar{f}_1 - \hat{b_{1i}}\bar{t}_i$$

where

$$S_{i_{tf_1}} = \sum t_i f_1 - \frac{\sum f_1 \sum t_i}{n}$$

and

$$S_{i_{t_i t_i}} = \sum t_i^2 - \frac{(\sum t_i)^2}{n}$$

where $n = 7$, $t = tr_i stg_j$ and tr_i is the resident time for drop of size i, meanwhile stg_j is the stage at j given data, for example $stg_2 = 7$. This method chooses the prediction $\hat{b_{1i}}$ that minimizes the sum of squared errors of prediction $\sum(f_1 - \hat{f}_1)^2$ for all sample points.

Table 3.2: The values of residence time and the slip velocity for each drop size

Drop Size(i)	0.0004	0.0011	0.0018	0.0025	0.0032	0.0039	0.0046	0.0053	0.0060	0.0067
Time(tr_i)	6.5225	2.9145	1.8427	1.5256	1.3760	1.2943	1.2487	1.3235	1.4257	1.5378
Velocity	0.0117	0.0261	0.0412	0.0498	0.0552	0.0587	0.0609	0.0574	0.0533	0.0494

Thus, by using this method, it is found that the concentration of the continuous phase depends on the function of time t, that is $f_{1i}(t) = a_{1i} + b_{1i}t$, where i corresponds to the different sizes of the drops and a_1 and b_1 are constants. The values of a_1 for the ten different sizes of drops are the same but the values of b_1 might differ according to drop sizes (refer Table 3.3). To find the best function which represents all the functions of t, the mean of the slopes of these linear functions is taken as the slope of the new function. This new function represents the relationship between the concentration of continuous phase and the resident time for all the 10 different drop sizes.

By assuming that the concentration on the surface of the drop is the same as the concentration of the continuous phase (the medium), we can use the new function $f_1(t)$ as the boundary condition of equation (3.1). Thus, we get a modified model of mass transfer of a single drop of which the boundary condition is a function of t, that is

$$f_1(t) = a_1 + b_1 t, \tag{3.32}$$

Table 3.3: The values of a_1 and b_1

a_1	b_1
0.9671	0.0304 $\times 10^{-}3$
0.9671	0.0681 $\times 10^{-}3$
0.9671	0.1077 $\times 10^{-}3$
0.9671	0.1301 $\times 10^{-}3$
0.9671	0.1442 $\times 10^{-}3$
0.9671	0.1533 $\times 10^{-}3$
0.9671	0.1589 $\times 10^{-}3$
0.9671	0.1499 $\times 10^{-}3$
0.9671	0.1392 $\times 10^{-}3$
0.9671	0.1290 $\times 10^{-}3$

3.3.1 The Analytical Solution

The constant concentration ac_0 in Equation (3.5) is now replaced by $f_1(t)$ from Equation (3.32), producing

$$u(a,t) = af_1(t), \quad t > 0, \tag{3.33}$$

while holding the other conditions unchanged. Rewrite Equations (3.3)-(3.6), where, we get IBVP of time-varying function boundary condition of

$$\begin{aligned}
\frac{\partial u}{\partial t} &= D\frac{\partial^2 u}{\partial r^2}, \quad 0 \leq r < a, \quad t \geq 0 && (3.34)\\
u(0,t) &= 0, \quad t > 0 && (3.35)\\
u(a,t) &= af_1(t) = f(t), \quad t > 0 && (3.36)\\
u(r,0) &= rc_1. \quad 0 \leq r < a && (3.37)
\end{aligned}$$

The solution of this IBVP with varied boundary condition for conduction of heat in solid is given by Carslaw and Jaeger in [38]. In this section, we show the detailed steps in order to get the solution of the problem. The method of separation of variables does not apply directly to the situation where time-varying boundary

condition arise. However, we show how by reformulating the problem it can be reduced to a nonhomogeneous diffusion equation.

Now, let the solution of these equations be

$$u(r,t) = U(r,t) + V(r,t), \tag{3.38}$$

substitute this equation into (3.34) and rearrange the terms to obtain

$$U_t(r,t) - DU_{rr}(r,t) = -[V_t(r,t) - DV_{rr}(r,t)].$$

The appropriate boundary conditions are then

$$\begin{aligned} U(0,t) &= -V(0,t), \quad t > 0 \\ U(a,t) &= f(t) - V(a,t), \quad t > 0 \end{aligned}$$

while the initial condition becomes

$$U(r,0) = rc_1 - V(r,0), \quad 0 \leq r < a.$$

The idea now is to make the boundary conditions for $U(r,t)$ homogeneous by making a suitable choice for $V(r,t)$. We will choose the simplest particular solution. This is accomplished by setting

$$V(r,t) = \frac{r}{a} f(t). \tag{3.41}$$

This choice for $V(r,t)$ converts the equation for $U(r,t)$, which is a nonhomogeneous diffusion equation, although now it is subject to the homogeneous boundary conditions. Rewrite IBVP of $U(r,t)$, we get

$$U_t - DU_{rr} = -\frac{r}{a} f'(t) \quad 0 \leq r < a, \quad t \geq 0 \tag{3.42}$$

$$U(0,t) = U(a,t) = 0, \quad t > 0 \tag{3.43}$$

$$U(r,0) = g(r) - \frac{r}{a} f(0), \quad 0 \leq r < a \tag{3.44}$$

where the related homogeneous problem is

$$v_t - Dv_{rr} = 0, \quad 0 \leq r < a, \quad t \geq 0 \tag{3.45}$$

$$v(0,t) = v(a,t) = 0, \quad t > 0 \tag{3.46}$$

$$v(r,0) = g(r) - \frac{r}{a} f(0), \quad 0 \leq r < a \tag{3.47}$$

The solution of (3.45)-(3.47) by the method of separation of variables is

$$v(r,t) = \sum_{n=1}^{\infty} A_n e^{\frac{-Dn^2\pi^2 t}{a^2}} \varphi_n(r), \tag{3.48}$$

where $A_n = \frac{2}{a}\int_0^a [g(r) - \frac{r}{a}f(0)] \sin\frac{n\pi r}{a}\ dr$ and $\varphi_n(r) = \sin\frac{n\pi r}{a}$.

The next step is to find a solution of the inhomogeneous problem of equations (3.42)-(3.47) in the form of a series like (3.48), but in which the parameters A_n are replaced by functions of t. The product $A_n e^{\frac{-Dn^2\pi^2 t}{a^2}}$ will then become a function $T_n(t)$ so that the solution will be a series

$$U(r,t) = \sum_{n=1}^{\infty} T_n(t)\varphi_n(r), \tag{3.49}$$

where

$$T_n(t) = \frac{2}{a}\int_0^a U(r,t)\varphi_n(r)\ dr. \tag{3.50}$$

We assume that $U_t(r,t)$ is a continuous function in the region $t > 0$, $0 \le r \le a$. Under these circumstances, the integral in (3.50) has a derivative with respect to t which can be calculated by differentiation under the integral sign. Referring to diffusion equation of (3.42)-(3.44), we get,

$$\begin{aligned} T_n'(t) &= \frac{2}{a}\int_0^a U_t(r,t)\varphi_n(r)\ dr. \\ &= \frac{2}{a}\int_0^a [DU_{rr}(r,t) - \frac{r}{a}f'(t)]\varphi_n(r)\ dr. \\ &= \frac{2D}{a}\int_0^a DU_{rr}(r,t)\varphi_n(r)\ dr - \frac{2}{a^2}f'(t)\int_0^a r\varphi_n(r)\ dr. \end{aligned} \tag{3.51}$$

The last term of (3.51), denoted as

$$q_n(t) = -\frac{2}{a^2}f'(t)\int_0^a r\varphi_n(r)\ dr,$$

is a known function since $-\frac{2}{a^2}f'(t)$ is given and using integration by parts we will get

$$\frac{2D}{a}\int_0^a U_{rr}(r,t)\varphi_n(r)\ dr = \frac{2D}{a}\int_0^a DU(r,t)\varphi_n''(r)\ dr.$$

Further because $\varphi_n'' = -\lambda^2\varphi_n$ and $\lambda = \frac{n\pi}{a}$

$$\begin{aligned} \frac{2D}{a}\int_0^a U_{rr}(r,t)\varphi_n(r)\ dr &= \frac{-2D}{a}\int_0^a \lambda^2 U(r,t)\varphi_n(r)\ dr \\ &= \frac{-2Dn^2\pi^2}{a^3}\int_0^a U(r,t)\varphi_n(r)\ dr, \end{aligned}$$

but from (3.50),

$$\frac{2D}{a}\int_0^a U_{rr}(r,t)\varphi_n(r)\ dr = -\frac{Dn^2\pi^2}{a^2}T_n(t) \tag{3.54}$$

and substitute (3.54) into (3.51), we get

$$\begin{aligned} T_n'(t) &= -\frac{Dn^2\pi^2}{a^2}T_n(t) + q_(t) \\ T_n'(t) + \frac{Dn^2\pi^2}{a^2}T_n(t) &= q_n(t) \end{aligned} \tag{3.55}$$

Equation (3.55) is a first-order linear differential equation where the integrating factor is $e^{\frac{Dn^2\pi^2 t}{a^2}}$. Therefore the solution of (3.55) is

$$T_n(t) = C_n e^{\frac{-Dn^2\pi^2 t}{a^2}} + \int_0^t e^{\frac{-Dn^2\pi^2(t-\tau)}{a^2}} q_n(\tau)\ d\tau. \tag{3.56}$$

Setting $t = 0$ in (3.50), we get the general equation of T_n, which is

$$\begin{aligned} T_n(0) = C_n &= \int_0^a U(r,0)\varphi_n(r)\ dr \\ &= \frac{2}{a}\int_0^a [g(r) - \frac{r}{a}f(0)]\sin\frac{n\pi r}{a}\ dr \\ &= \frac{2}{a}\int_0^a g(r)\sin\frac{n\pi r}{a}\ dr + \frac{2}{n\pi}(-1)^n f(0), \end{aligned} \tag{3.57}$$

and

$$q_n(t) = \frac{2}{n\pi}f'(t)(-1)^n. \tag{3.58}$$

The coefficient $T_n(t)$ in (3.49) are completely known and hence problem (3.42)-(3.44) has been solved. We have

$$\begin{aligned} U(r,t) &= \frac{2}{a}\sum_{n=1}^{\infty} e^{\frac{-Dn^2\pi^2 t}{a^2}}\sin\frac{n\pi r}{a}\left(\int_0^a g(r)\sin\frac{n\pi r}{a}\ dr\right) + \\ &\quad \frac{2}{\pi}f(0)\sum_{n=1}^{\infty}\frac{(-1)^n}{n}e^{\frac{-Dn^2\pi^2 t}{a^2}}\sin\frac{n\pi r}{a} + \\ &\quad \frac{2}{\pi}\sum_{n=1}^{\infty}\frac{(-1)^n}{n}e^{\frac{-Dn^2\pi^2 t}{a^2}}\sin\frac{n\pi r}{a}\left(\int_0^t f'(\tau)e^{\frac{Dn^2\pi^2\tau}{a^2}}\ d\tau\right). \end{aligned}$$

From (3.41) and $u(r,t) = V(r,t) + U(r,t)$, the solution for diffusion equation of (3.34)-(3.37) is

$$\begin{aligned} u(r,t) &= \frac{r}{a}f(t) + \frac{2}{a}\sum_{n=1}^{\infty} e^{\frac{-Dn^2\pi^2 t}{a^2}}\sin\frac{n\pi r}{a}\left(\int_0^a g(r)\sin\frac{n\pi r}{a}\ dr\right) + \\ &\quad \frac{2}{\pi}f(0)\sum_{n=1}^{\infty}\frac{(-1)^n}{n}e^{\frac{-Dn^2\pi^2 t}{a^2}}\sin\frac{n\pi r}{a} + \\ &\quad \frac{2}{\pi}\sum_{n=1}^{\infty}\frac{(-1)^n}{n}e^{\frac{-Dn^2\pi^2 t}{a^2}}\sin\frac{n\pi r}{a}\left(\int_0^t f'(\tau)e^{\frac{Dn^2\pi^2\tau}{a^2}}\ d\tau\right). \end{aligned}$$

By taking $f(t) = a_1 + b_1 t$ which gives us

$$\int_0^t f'(\tau) e^{\frac{Dn^2\pi^2\tau}{a^2}}\, d\tau = b_1 \left(\frac{a^2}{Dn^2\pi^2} e^{\frac{Dn^2\pi^2 t}{a^2}} - \frac{a^2}{Dn^2\pi^2} \right)$$

and also we know that from the initial condition $g(r) = c_1 r$ which resulted in

$$\int_{r=0}^{r=t} g(r) \sin \frac{n\pi r}{a} dr = c_1 \big(\frac{-a^2}{n\pi} (-1)^n \big),$$

then

$$\begin{aligned} u(r,t) &= \frac{r}{a}(a_1 + b_1 t) + \frac{2c_1 a}{\pi} \sum_{n=1}^{\infty} \frac{(-1)^{n+1}}{n} e^{\frac{-Dn^2\pi^2 t}{a^2}} \sin \frac{n\pi r}{a} + \\ & \frac{2a_1}{\pi} \sum_{n=1}^{\infty} \frac{(-1)^n}{n} e^{\frac{-Dn^2\pi^2 t}{a^2}} \sin \frac{n\pi r}{a} - \\ & \frac{2b_1 a^2}{D\pi^3} \sum_{n=1}^{\infty} \frac{(-1)^{n+1}}{n^3} \sin \frac{n\pi r}{a} + \\ & \frac{2b_1 a^2}{D\pi^3} \sum_{n=1}^{\infty} \frac{(-1)^{n+1}}{n^3} e^{\frac{-Dn^2\pi^2 t}{a^2}} \sin \frac{n\pi r}{a} \end{aligned} \tag{3.60}$$

Knowing that

$$\sum_{1}^{\infty} \frac{(-1)^{n+1}}{n^3} \sin \frac{n\pi r}{a} = -\frac{(r^3 - a^2 r)\pi^3}{12a^3},$$

substituting this equation into (3.60) and rearranging them , give us

$$\begin{aligned} u(r,t) &= \frac{r}{a}(a_1 + b_1 t) + \frac{b_1}{6Da}(r^3 - a^2 r) + 2\frac{c_1 a - a_1}{\pi} \sum_{1}^{\infty} \frac{(-1)^{n+1}}{n} e^{\frac{-Dn^2\pi^2 t}{a^2}} \sin \frac{n\pi r}{a} + \\ & \frac{2b_1 a^2}{D\pi^3} \sum_{1}^{\infty} \frac{(-1)^{n+1}}{n^3} e^{\frac{-Dn^2\pi^2 t}{a^2}} \sin \frac{n\pi r}{a}. \end{aligned} \tag{3.61}$$

Thus the solution of the diffusion equation of (3.1) with respect to the initial-boundary condition of Equations (3.35), (3.36) and (3.37) is

$$\begin{aligned} C(r,t) &= \frac{1}{a}(a_1 + b_1 t) + \frac{b_1}{6Da}(r^2 - a^2) + 2\frac{c_1 a - a_1}{\pi r} \sum_{1}^{\infty} \frac{(-1)^{n+1}}{n} e^{\frac{-Dn^2\pi^2 t}{a^2}} \sin \frac{n\pi r}{a} + \\ & \frac{2b_1 a^2}{D\pi^3 r} \sum_{1}^{\infty} \frac{(-1)^{n+1}}{n^3} e^{\frac{-Dn^2\pi^2 t}{a^2}} \sin \frac{n\pi r}{a}. \end{aligned} \tag{3.62}$$

As mentioned in the previous section, we are interested in the average concentration of the sphere, C_{av}, given by Equation (3.23). Substituting (3.62) into

(3.24), we get

$$\begin{aligned} C_t &= \int_{r=0}^{r=a} \big[\frac{1}{a}(a_1+b_1t)+\frac{b_1}{6Da}(r^2-a^2)\big]4\pi r^2\ dr + \\ &\int_{r=0}^{r=a} \big[2\frac{c_1a-a_1}{\pi r}\sum_1^\infty \frac{(-1)^{n+1}}{n}e^{\frac{-Dn^2\pi^2t}{a^2}}\sin\frac{n\pi r}{a}\big]4\pi r^2\ dr + \\ &\int_{r=0}^{r=a} \big[\frac{2b_1a^2}{D\pi^3 r}\sum_1^\infty \frac{(-1)^{n+1}}{n^3}e^{\frac{-Dn^2\pi^2t}{a^2}}\sin\frac{n\pi r}{a}\big]4\pi r^2\ dr \qquad (3.63) \\ &= A+B+E \qquad (3.64) \end{aligned}$$

where

$$\begin{aligned} A &= \int_{r=0}^{r=a} \big[\frac{1}{a}(a_1+b_1t)+\frac{b_1}{6Da}(r^2-a^2)\big]4\pi r^2\ dr \\ &= \frac{4}{3}\pi a^2(a_1+b_1t)-\frac{4\pi b_1a^4}{45D}, \\ B &= \int_{r=0}^{r=a} \big[2\frac{c_1a-a_1}{\pi r}\sum_1^\infty \frac{(-1)^{n+1}}{n}e^{\frac{-Dn^2\pi^2t}{a^2}}\sin\frac{n\pi r}{a}\big]4\pi r^2\ dr \\ &= \frac{8a^2(c_1a-a_1)}{\pi}\sum_1^\infty \frac{1}{n^2}e^{\frac{-Dn^2\pi^2t}{a^2}}, \\ E &= \int_{r=0}^{r=a} \big[\frac{2b_1a^2}{D\pi^3 r}\sum_1^\infty \frac{(-1)^{n+1}}{n^3}e^{\frac{-Dn^2\pi^2t}{a^2}}\sin\frac{n\pi r}{a}\big]4\pi r^2\ dr \\ &= \frac{8b_1a^4}{D\pi^3}\sum_1^\infty \frac{1}{n^4}e^{\frac{-Dn^2\pi^2t}{a^2}}. \end{aligned}$$

Thus the average concentration C_{av} of the sphere is

$$\begin{aligned} C_{av} &= \frac{(a_1+b_1t)}{a}-\frac{b_1a}{15D}+\frac{6(c_1a-a_1)}{\pi^2a}\sum_1^\infty \frac{1}{n^2}e^{\frac{-Dn^2\pi^2t}{a^2}}+ \\ &\frac{6b_1a}{D\pi^4}\sum_1^\infty \frac{1}{n^4}e^{\frac{-Dn^2\pi^2t}{a^2}}. \qquad (3.65) \end{aligned}$$

Following with this result, we derive the new fractional approach to equilibrium based on Equation (3.25), as

$$F_{new}(t)=\frac{C_{av}-c_1}{f(t)/a-c_1} \qquad (3.66)$$

where $f(t)/a$ and c_1 are the boundary condition and initial condition of IBVP of equation (3.1) respectively. By substituting (3.65) into (3.66), we get

$$\begin{aligned} F_{new} &= \frac{(a_1+b_1t)}{a(a_1+b_1t-c_1)}-\frac{b_1a}{15D(a_1+b_1t-c_1)}+ \\ &\frac{6(c_1a-a_1)}{\pi^2a(a_1+b_1t-c_1)}\sum_1^\infty \frac{1}{n^2}e^{\frac{-Dn^2\pi^2t}{a^2}}+ \\ &\frac{6b_1a}{D\pi^4(a_1+b_1t-c_1)}\sum_1^\infty \frac{1}{n^4}e^{\frac{-Dn^2\pi^2t}{a^2}}- \\ &\frac{c_1}{(a_1+b_1t-c_1)}. \qquad (3.67) \end{aligned}$$

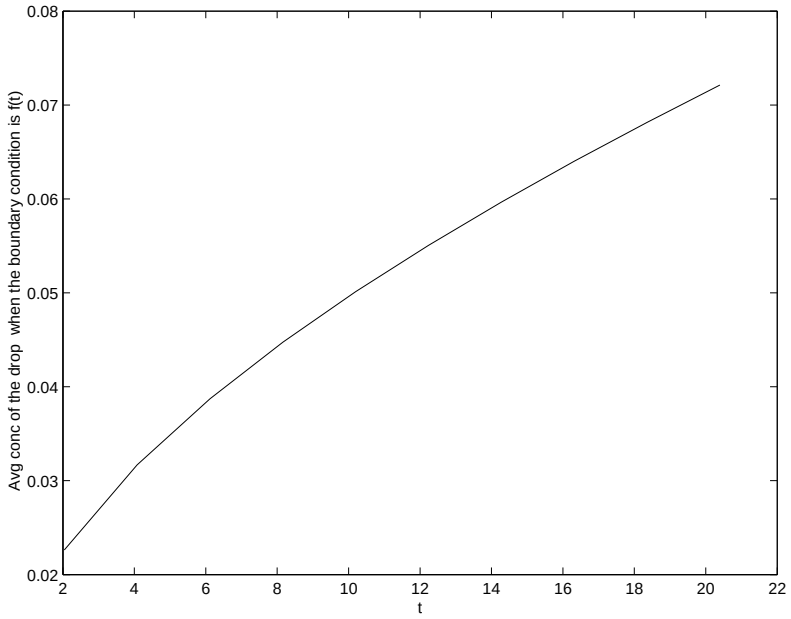

Figure 3.2: Sorption curve for sphere with surface concentration $a_1 + b_1 t$

3.4 Simulations for Different Drop Sizes

We consider the drop of size $0.00705m$ in diameter. The time taken for the drop to move upwards in one compartment is 0.8868 seconds. From the least square method, we found that $f_1(t)$ is equal to $0.9187 + 0.0041t$. Then let $f(t) = a_1 + b_1$ where $a_1 = a(0.9187)$ and $b_1 = a(0.0041)$. Substitute this value and all the parameters into (3.65) and we will get the relationship between the average concentration of the sphere and the time, t. The relationship can easily be seen in Figure 3.2.

The comparison between this fractional approach to equilibrium, $F_{new}(t)$ and the one obtained by Talib[4] is made based on the graph plotted in Figure 3.3. In addition, simulations are also carried out to see the effect on fractional approach to equilibrium with variations in drop sizes. A graphical representation of the effect of variations in drop sizes is shown in Figure 3.4.

The concentration profiles of the curves shown in Figure 3.4 show that smaller drops reach equilibrium concentration with the medium at a much faster rate than larger drops. The profile of fractional approach to equilibrium of the modified model compared with Crank's[7] and Vermuelen's[35] is similar.

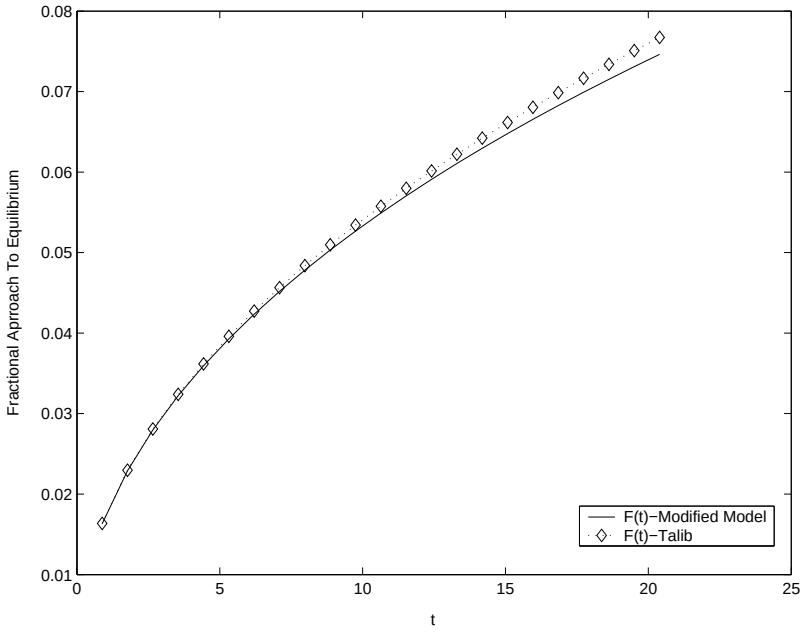

Figure 3.3: Fractional approach to equilibrium vs. time

3.5 Discussion and Conclusion

In this chapter the modified mass transfer model was formulated based on experimental data. By least square method and the assumption that the concentration on the surface of the drop is the same as the concentration of the continuous phase, the boundary condition of the IBVP was found to be a time dependent function, $f_1(t) = a_1 + b_1(t)$. The analytical solution of the model was then detailed in Section 3.3.1. This was followed by the derivation of the new fractional approach to equilibrium.

For comparison purposes, the new fractional approach to equilibrium profiles of the time-dependent boundary condition and that of Talib[4] are shown in Figure 3.3. Although the model considered here is a modification of the model proposed by Talib[4], the new fractional approach to equilibrium profile agrees with the result obtained by Talib. In conclusion, the new fractional approach to equilibrium gives a better theory for further investigation of the mass transfer process in the RDC column. This is because the new term was derived from the time-dependent boundary condition which represents the real phenomena of the process in the column.

For further analysis, the simulations with variations in drop sizes were also carried out to see their effect on the new fractional approach to equilibrium. From Figure 3.4, the smaller the drop,the equilibrium concentration is more rapidly attained

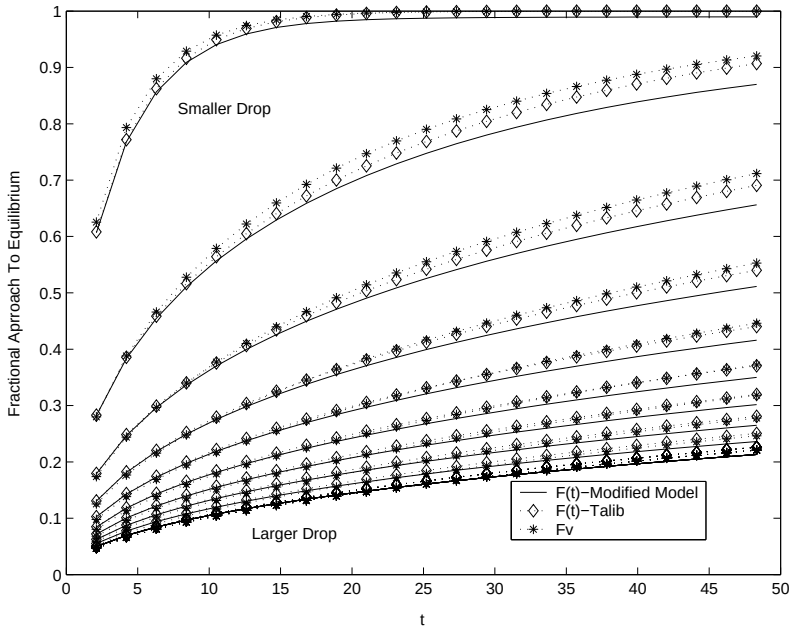

Figure 3.4: Fractional Approach to equilibrium vs. time for different drop sizes

. This is due to the fact that the smaller drop provides larger surface area to the volume ratio, which causes a better absorption of the mass from the continuous phase.

The IBVP given by Equations (3.3), (3.4), (3.6) and (3.32) holds for a non-moving drop in a stagnant medium. In a real RDC column drops are rising or falling in the continuous phase, which induces internal circulation. The internal circulation has the effect of distributing the solute uniformly in the drop to give the drop a uniform concentration as it moves to the exit point. Therefore the following chapter will discuss the mass transfer model of a moving drop in a non-stagnant medium.

CHAPTER 4

MASS TRANSFER IN THE MULTI-STAGE RDC COLUMN

4.1 Introduction

In the previous chapter we have shown the development of the modified mass transfer model of time-dependent boundary value problem (BVP). The model involved only the mass transfer of a single drop in a stagnant medium. The profile of the fractional approach to equilibrium of the modified model agrees with the model introduced by Talib[4] and Vermuelen[35].

Since in the RDC column the drops are moving in the continuous phase with counter current direction, the mass transfer model of a moving drop in a non-stagnant medium will be considered here. The new fractional approach to equilibrium is also incorporated in developing the model.

According to the two-film theory, the concentrations of the two phases at an interface where the equilibrium exist, is governed by the principles of physical equilibrium. Due to this phenomenon at the interface, the boundary condition given by Equation (3.36) has to be redefined. In the following section the IBVP with new boundary condition will be given. In this section, the mass transfer model based on modified quadratic driving force which is called *Time-dependent Quadratic Driving Force(TQDF)* is described. Based on this model, we design a Mass Transfer of A Single Drop Algorithm. This is then followed by a more realistic Mass Transfer of Multiple Drops Algorithm. For comparison purposes, a normalization and the de-normalization

techniques are given in Section 4.5.

An alternative method of calculating the mass transfer for a Multi-Stage System is also presented in the form of an algorithm named as the Mass Transfer Steady State Algorithm. Finally, a discussion about the models is also presented.

4.2 The Diffusion Process Based On The Concept Of Interface Concentration

Consider the previous IBVP. The diffusion process based on the concept of interface concentration is obtained by replacing Equation (3.32) with the interface condition. Then we get

$$\frac{\partial u}{\partial t} = D\frac{\partial^2 u}{\partial r^2}, \quad 0 \leq r < a, \quad t \geq 0 \tag{4.1}$$

$$u_s(a,t) = f(c_s), \quad t \geq 0 \tag{4.2}$$

$$u(r,0) = rc_1, \quad 0 \leq r < a \tag{4.3}$$

where u_s is the drop surface concentration, c_s is the concentration of medium at the drop surface and $u_s(a,t) = f(c_s)$ is known as the equilibrium equation, which expresses the concentration of the drop in equilibrium with the medium at the drop surface.

A drop with concentration cd_{in_1} entering a column is subjected to the concentration of the first compartment, cc_1. Solutes from the continuous phase are transferred to the drop. Now the concentration of the drop is cd_{out_1}. On reaching the next compartment, the drop concentration, cd_{in_2}, where $cd_{in_2} = cd_{out_1}$, is now in a continuous phase concentration of the second compartment, cc_2, then the drop concentration, cd_{out_2} after leaving the second compartment can be obtained. By applying the same approach to the drop as it moves through every compartment, the drop concentration cd_{out_n} at the final compartment, cc_n can be determined.

The mass transfer model based on the linear driving force is realistic if the interface of the two liquids in contact is a simple plane. In 1953, Vermuelen[35] had shown that if one of the interfaces of the two liquids is spherical, than the driving

force in a drop can be considered as non-linear. His expression known as *quadratic driving force* was used successfully by previous researcher as can be found in [4]. In this study we used the same concept and the new fractional approach to equilibrium is also incorporated into the idea to get a new driving force named as *Time Dependent Quadratic Driving Force(TQDF).*

The following section explains the rate of the mass transfer or flux across the drop surface into the drop where the derivation of the time dependent quadratic driving force is shown.

4.2.1 Flux Across The Drop Surface Into The Drop

The rate of mass transfer across the surface of the sphere given by flux J is defined as

$$Ja_p = \frac{dC}{dt}, \tag{4.4}$$

where a_p is considered as ratio of the surface area to the volume of a drop. From Equation (3.66) the fractional approach to equilibrium of the new model is

$$F_{new}(t) = \frac{C_{av} - c_1}{f_1(t) - c_1}$$

and since the profile of fractional approach to equilibrium of the modified model is similar to that of Crank[7] and Vermuelen[35] , we replace $F_{new}(t)$ with the one used by Vermuelen that is

$$F_v = (1 - e^{-D\pi^2 t/a^2})^{0.5}. \tag{4.6}$$

Thus, Equation (3.66) becomes

$$F_v = \frac{C_{av} - c_1}{f_1(t) - c_1} \tag{4.7}$$

Differentiating the above equation with respect to t, gives us

$$\begin{aligned} \frac{d}{dt}(F_v) &= \frac{d}{dt}(\frac{C_{av} - c_1}{f_1(t) - c_1}), \\ \frac{1}{2}(\frac{D\pi^2}{a^2})(\frac{1 - F_v^2(t)}{F_v(t)}) &= \frac{1}{f_1(t) - c_1}\frac{d}{dt}(C_{av}) - \frac{C_{av} - c_1}{(f_1(t) - c_1)^2}\frac{d}{dt}f_1(t) \end{aligned} \tag{4.8}$$

By taking F_v as (4.7) and rewriting, Equation (4.8) becomes,

$$\frac{d}{dt}(C_{av}) = \frac{1}{2}\frac{D\pi^2}{a^2}\frac{(f_1(t)-c_1)^2-(C_{av}-c_1)^2}{(C_{av}-c_1)} + \frac{(C_{av}-c_1)}{(f_1(t)-c_1)}\frac{d}{dt}f_1(t) \tag{4.9}$$

Substituting this equation into (4.4) and rearranging them, gives us

$$\begin{aligned} J &= \frac{1}{2a_p}\frac{D\pi^2}{a^2}\left(\frac{(f_1(t)-c_1)^2-(C_{av}-c_1)^2}{C_{av}-c_1}\right) + \frac{1}{a_p}\frac{C_{av}-c_1}{(f_1(t)-c_1)}\frac{d}{dt}f_1(t) \\ &= \frac{4}{2a_p}\frac{D\pi^2}{d^2}\left(\frac{(f_1(t)-c_1)^2-(C_{av}-c_1)^2}{C_{av}-c_1}\right) + \frac{1}{a_p}\frac{C_{av}-c_1}{(f_1(t)-c_1)}\frac{d}{dt}f_1(t) \\ &= \frac{1}{3}\frac{D\pi^2}{d}\left(\frac{(f_1(t)-c_1)^2-(C_{av}-c_1)^2}{C_{av}-c_1}\right) + \frac{d}{6}\frac{C_{av}-c_1}{(f_1(t)-c_1)}\frac{d}{dt}f_1(t) \end{aligned} \tag{4.10}$$

where $a_p = \frac{6}{d}$. The term $\left(\frac{(f_1(t)-c_1)^2-(C_{av}-c_1)^2}{C_{av}-c_1}\right)$ is known as the time-dependent quadratic driving force. In this study, the quadratic driving force term is different from the one used by Talib[4]. Here, $f_1(t)$ is taken to be the surface concentration of the drop instead of a constant, c_0 which is used by Talib.

The rate of the mass transfer from the bulk concentration of the continuous phase to the surface is given in the following section.

4.2.2 Flux in the Continuous Phase

The flux transfer in the continuous phase is given by

$$J = k_c(c_b - c_s), \tag{4.11}$$

where k_c is the film mass transfer coefficient of the continuous phase. c_b is the bulk concentration in the continuous phase and c_s is the concentration at the interface. $(c_b - c_s)$ is the linear concentration driving force from the continuous bulk concentration to the drop surface.

4.2.3 Process of Mass Transfer Based on Time-dependent Quadratic Driving Force

The mass transfer across the surface of the sphere given by flux J defined in Equation (4.10) where $(\frac{(f_1(t)-c_1)^2-(C_{av}-c_1)^2}{C_{av}-c_1})$ is called the time-dependent quadratic driving force. Meanwhile the flux transfer in the continuous phase is given by (4.11). As stated before, at the interface, (4.10) and (4.11) are equal, that is

$$\frac{1}{3}\frac{D_y\pi^2}{d}(\frac{(f_1(t)-c_1)^2-(C_{av}-c_1)^2}{C_{av}-c_1})+\frac{d}{6}\frac{C_{av}-c_1}{(f_1(t)-c_1)}\frac{d}{dt}f_1(t)=k_c(c_b-c_s), \quad (4.12)$$

where D_y is the molecular diffusivity in the drop phase. By substituting (4.7) into (4.12), we will get

$$\frac{D_y\pi^2}{3d}(f_1(t)-c_1)(\frac{1-F_v(t)^2}{F_v(t)})+\frac{d}{6}F_v(t)\frac{1}{dt}f_1(t)=k_c(c_b-c_s). \quad (4.13)$$

In this work, the concentration of both phases is in a normalized form that is, the concentration is dimensionless which lies in the interval between zero and one. For simplicity and to differentiate the latter terms from the original terms, we denote C_{av}, c_1, $f_1(t)$, c_b and c_s as y_{av}, y_0, y_s, x_b and x_s respectively. Then (4.13) becomes

$$\frac{D_y\pi^2}{3d}(y_s-y_0)(\frac{1-F_v(t)^2}{F_v(t)})+\frac{d}{6}F_v(t)\frac{1}{dt}f_1(t)=k_x(x_b-x_s). \quad (4.14)$$

By rearranging this equation, we get

$$y_s=\frac{3d}{D\pi^2}k_x(x_b-x_s)\frac{F_v}{1-F_v^2}-(\frac{3d}{D_y\pi^2})(\frac{F_v}{1-F_v^2})(\frac{d}{6})F_v(t)\frac{1}{dt}f_1(t)+y_0 \quad (4.15)$$

Now, consider the situation at the drop surface. Equilibrium between the medium and the concentration of drop is governed by equation

$$y_s=f(x_s), \quad (4.16)$$

where for Cumene/Iso-butyric acid/Water system $f(x_s)=x_s^{1.85}$.

The drop and medium concentrations, y_s and x_s, at the surface are found by solving the non-linear equations of (4.15) and (4.16). In order to solve these equations, we used bisection method. First, we substitute (4.16) into (4.15) which give us

$$\begin{aligned} x_s^{1.85} &= \frac{3d}{D\pi^2}k_x(x_b - x_s)\frac{F_v}{1-F_v^2} - (\frac{3d}{D_y\pi^2})(\frac{F_v}{1-F_v^2})(\frac{d}{6})F_v(t)\frac{1}{dt}f_1(t) + y_0 \\ 0 &= \frac{3d}{D\pi^2}k_x(x_b - x_s)\frac{F_v}{1-F_v^2} - (\frac{3d}{D_y\pi^2})(\frac{F_v}{1-F_v^2})(\frac{d}{6})F_v(t)\frac{1}{dt}f_1(t) + y_0 - x_s^{1.85}. \end{aligned}$$

Then let

$$g(x_s) = \frac{3d}{D\pi^2}k_x(x_b - x_s)\frac{F_v}{1-F_v^2} - (\frac{3d}{D_y\pi^2})(\frac{F_v}{1-F_v^2})(\frac{d}{6})F_v(t)\frac{1}{dt}f_1(t) + y_0 - x_s^{1.85}. \quad (4.17)$$

With the assumption that the values of y_s and x_s lie between 0 and 1, the root of Equation (4.17) must lie in the interval $[0, 1]$. Let the root be c, then by the bisection method we get $c = \frac{0+1}{2}$. This value is then substituted into Equation (4.17). If $g(c = 1/2) = 0$ then the root of g is $c = 1/2$. Otherwise we have to repeat the process of determining the value of c by checking the values of $(g(0) \times g(1/2))$ and $(g(1) \times g(1/2))$. If $(g(0) \times g(1/2)) < 0$ set $a = 0$ and $b = 1/2$, then $c = \frac{0+1/2}{2}$. If $g(1) \times g(1/2) < 0$ set $a = 1/2$ and $b = 1$ then $c = \frac{1/2+1}{2}$. With these values, repeat the process until the root of g is obtained. These steps are well presented in the algorithm below.

Bisection Algorithm

The following algorithm is used to calculate x_s.

Step 1: Choose the initial solution of g, c, to lie in the interval $[a, b]$ and initialize it to $\frac{a+b}{2}$. Set $i = 1$.

Step 2: Calculate the values of $g(a_i)$, $g(b_i)$ and $g(c_i)$ using Equation (4.17).

Step 3: If $g(c_i) \leq 0.00001$, set $c = c_i$ and stop.

else go to Step 4.

Step 4: If $(g(a_i) \times g(c_i)) < 0$ set $i = i + 1$, $a_{i+1} = a_i$, $b_{i+1} = c_i$ and $c_{i+1} = \frac{a_i+c_i}{2}$, then repeat Steps 2 to 3,

else if $(g(a_i) \times g(b_i)) < 0$ set $a_{i+1} = c_i$, $b_{i+1} = b_i$ and $c_{i+1} = \frac{c_i+b_i}{2}$, then repeat Steps 2 to 3.

The value of x_s is substituted into Equation (4.15) or (4.16) to obtain y_s. This value is then used to calculate the average concentration of the drop using equation,

$$y_{av} = F_{new}(t)(y_s - y_0) + y_0, \tag{4.18}$$

where $F_{new}(t)$ is the new fractional approach to equilibrium. Then the amount of mass transfer of the drops can be obtained by applying mass balance equation, that is

$$F_x(x_{in} - x_{out}) = F_y(y_{out} - y_{in}), \tag{4.19}$$

where F_x and F_y are the flow rates of the continuous phase and the dispersed phase respectively. The concentrations x_{in} and y_{in} are the uniform initial concentrations of the continuous and drop phase. In this case x_{in} and y_{in} are x_b and y_0 respectively. Meanwhile x_{out} and y_{out} are the exit concentration of the continuous and drop phase respectively where we take y_{av} as y_{out}.

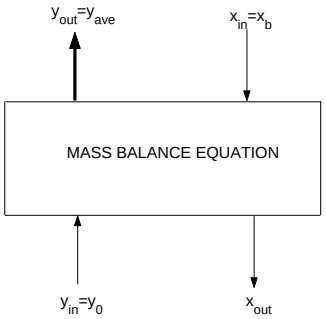

Figure 4.1: Schematic diagram to explain the mass balance process

Equations (4.15)-(4.19) are used to calculate the amount of mass transfer from the continuous phase to the drop. Based on various studies [17, 20, 27], the process in the RDC column is very complicated because it involves not only mass transfer of a single drop but infinitely many drops. These drops have different sizes and different velocities. In this work we modelled the distribution of the drops along the column exactly according to the model discussed by Arshad[6].

Before we construct a model that describes the mass transfer process as close as the real process, the following section will explain the process of the mass transfer of only a single drop with known size in the multi-stage RDC column.

4.3 Mass Transfer of a Single Drop

In this section, the process of the mass transfer of a single drop in the continuous unsteady state medium of the 23 stages RDC column is considered. As explained in the previous section, each compartment in the RDC column corresponds to the stage number. The model concerns the mass transfer process of a single drop in every compartment, where each compartment has its own medium concentration.

In this model, we assume that the continuous phase is continuously flowing in the column with a unit concentration. Then a drop is injected into the column with zero concentration. We also assume that the mass transfer takes place only when the drop reaches the first compartment. Here the new fractional approach to equilibrium is used, which is based on Equation (3.66) where the equation of average concentration of the drop C_{av}, is given by (3.65) such that the new fractional approach to equilibrium is (3.67).

The time t given in the Equation (3.67) is replaced with residence time $t_{r,i}$ of a particular drop i in a compartment. Using this residence time and Equations (4.15)-(4.19), the drop concentration in the first compartment is obtained. This concentration is then taken as the initial concentration of the drop as the drop enters the second compartment. This process is repeated through the final stage. The second drop is then injected into the column with zero concentration but this time the concentration of the medium, x_{out} as calculated in the first batch of the process is used. We stop the simulation when the steady state of the concentration of the drop at every compartment is reached. In other words, the simulation is completed when the difference between the concentration at iteration t and iteration $t-1$ is very small. This condition must be satisfied at each compartment.

The model described above is presented in Subsection 4.3.1.

4.3.1 Algorithm 4.1: Algorithm for Mass Transfer Process of a Single Drop (MTASD Algorithm)

The process of mass transfer will continuously take place until the concentration of the continuous phase is in equilibrium with the surface concentration of the drop. The algorithm below describes the detail of the process of the mass transfer from stage 1 up to stage 23 for a single drop.

Algorithm to find the concentration of the liquids after the extraction process of a single drop in 23 stages RDC Column.

This algorithm calculates the amount of the mass transfer from the continuous phase to the drop.

Step 1: Input all the geometrical details and physical properties of the system. Set $i_{itr} = 1$, $x_{in} = 1$ and $y_{in} = 0$.

Step 2: Input initial values, that is x_{in} and y_{in}. Set $j = 1$ (stage 1)

Step 3: Calculate the value of fractional approach to equilibrium based on Varmulene Equation (4.6) and the new Equation (3.67) which was based on the varied boundary condition.

Step 4: Calculate the surface concentration of the medium and drop, x_s and y_s respectively by solving the non-linear equations (4.15) and (4.16). Assume the bulk concentration of the medium, x_b is x_{in} and the initial drop concentration, y_0 is y_{in}.

Step 5: If $y_s > y_{in}$ go to Step 6 **else**, set $y_{out} = y_{in}$, then go to Step 7.

Step 6: Determine the average concentration of the drops using Equation (4.18). This value is taken to be the output concentration of the drop at jth stage, y_{out}.

Step 7: Determine the concentration of the medium at the jth stage by using mass balance equation of (4.19). This value is taken to be x_{out} at the jth stage.

Step 8: If $j > 23$ go to Step 10,

else go to Step 9.

Step 9: Update the initial value for the next stage.

9a: If $i_{itr} = 1$, set $x_{in} = 1$, $y_{in} = y_{out}(i_{itr}, j)$, $\forall j = 1, 2, ...n$

else go to 9b.

9b: If $j \leq n - 2$ set $x_{in} = x_{out}(i_{itr} - 1, j + 2)$ and $y_{in} = y_{out}(i_{itr}, j)$,

else $(j = n - 1)$ set $x_{in} = 1$, $y_{in} = y_{out}(i_{itr}, j)$.

Set $j = j + 1$. Repeat Steps 3 to 8.

Step 10: Take $\epsilon = 0.0001$. If $|y_{out}(i_{itr}, j) - y_{out}(i_{itr} - 1, j)| \leq \epsilon$, stop, **else** go to Step 11.

Step 11: Update the initial value for the next i_{itr}.

11a: Start with $i_{itr} = 1$ set $x_{in} = x_{out}(i_{itr}, j = 2)$, $y_{in} = 0$

11b: $i_{itr} = i_{itr} + 1$ set $x_{in} = x_{out}(i_{itr}, j = 2)$, $y_{in} = 0$ $\forall i_{itr} = 2, 3, 4, ...$

Set $i_{itr} = i_{itr} + 1$. Repeat Steps 2 to 10.

Figure 4.2 is the schematic representation of the mass transfer process of a single drop in 23 stages RDC column in the form of a flow chart.

4.3.2 Simulation Results

Using Algorithm 4.1, we run the program to produce simulation results of the mass transfer process for a single drop in a 23 stage RDC column. The profile concentrations of continuous and dispersed phase along the column are shown in Figure 4.3. For comparison purposes we also plot the concentrations of the continuous and dispersed phase based on the new mass transfer model and Crank solution as seen in Figure 4.4. Simulations were also carried out for different drop sizes. The concentrations of the drop of different drop sizes are shown in Table 4.1.

4.4 Mass Transfer of Multiple Drops

In a real RDC column, the dispersed phase is injected into the column in the form of drops. These drops will rise up the column if their density is less than that of

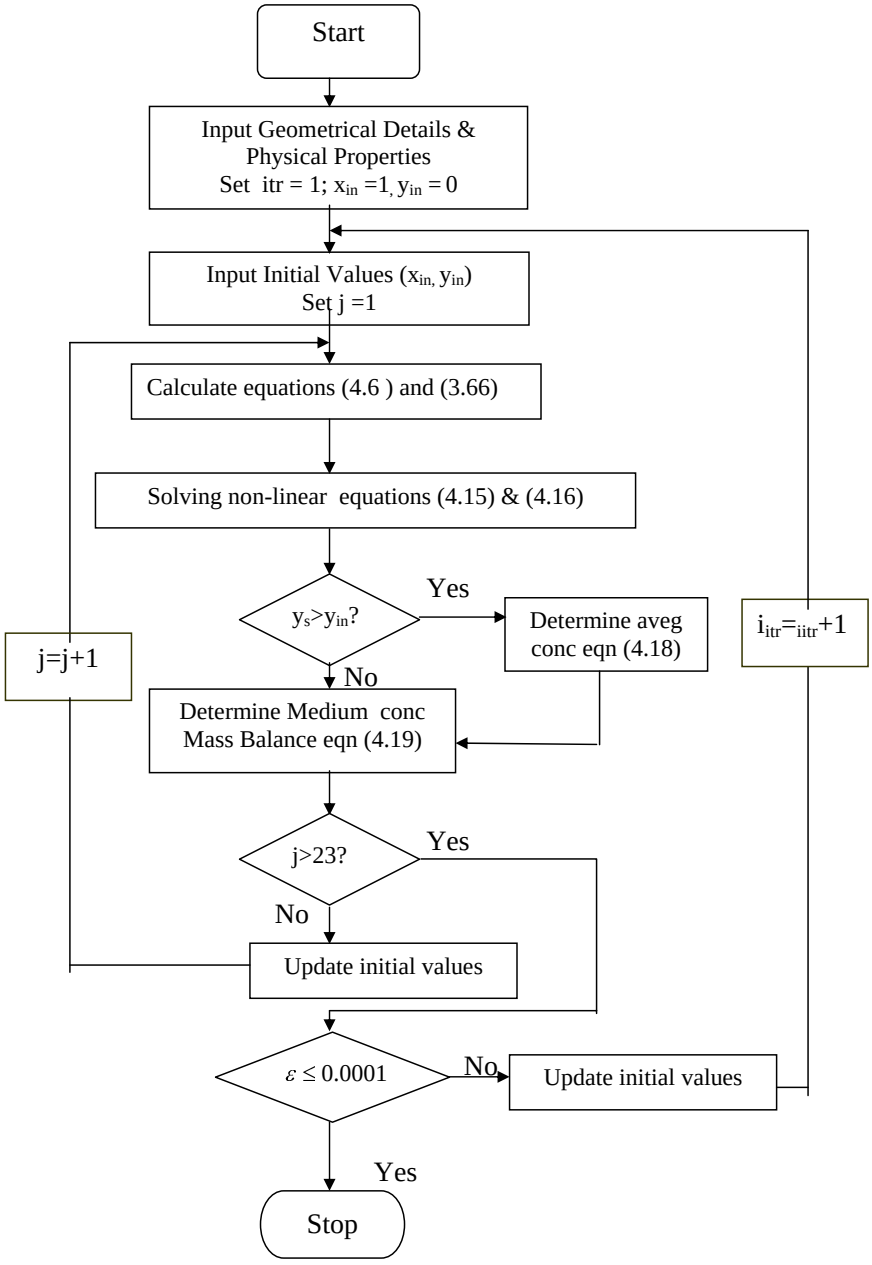

Figure 4.2: Flow chart of mass transfer process in the 23-stage RDC column for MTASD Algorithm

Table 4.1: The concentration of the drops along the column

Stage No	Drop size									
	d_1	d_2	d_3	d_4	d_5	d_6	d_7	d_8	d_9	d_{10}
1	0.043	0.0093	0.0039	0.0026	0.0021	0.0018	0.0017	0.0017	0.0017	0.0017
2	0.0831	0.0185	0.0078	0.0051	0.0041	0.0036	0.0034	0.0034	0.0034	0.0034
3	0.1206	0.0275	0.0117	0.0077	0.0062	0.0054	0.0051	0.005	0.0051	0.0051
4	0.156	0.0364	0.0155	0.0102	0.0082	0.0072	0.0067	0.0067	0.0068	0.0069
5	0.1894	0.0452	0.0194	0.0128	0.0102	0.009	0.0084	0.0083	0.0084	0.0086
6	0.221	0.0538	0.0232	0.0153	0.0123	0.0108	0.0101	0.01	0.0101	0.0103
7	0.251	0.0624	0.0269	0.0178	0.0143	0.0126	0.0117	0.0117	0.0118	0.0119
8	0.2795	0.0708	0.0307	0.0203	0.0163	0.0144	0.0134	0.0133	0.0134	0.0136
9	0.3066	0.0792	0.0344	0.0228	0.0183	0.0162	0.015	0.0149	0.0151	0.0153
10	0.3326	0.0874	0.0381	0.0253	0.0203	0.018	0.0167	0.0166	0.0167	0.017
11	0.3573	0.0955	0.0418	0.0278	0.0223	0.0197	0.0183	0.0182	0.0184	0.0187
12	0.3809	0.1035	0.0455	0.0302	0.0243	0.0215	0.02	0.0198	0.02	0.0203
13	0.4036	0.1115	0.0491	0.0327	0.0263	0.0232	0.0216	0.0215	0.0217	0.022
14	0.4252	0.1193	0.0528	0.0351	0.0283	0.025	0.0232	0.0231	0.0233	0.0237
15	0.446	0.1271	0.0564	0.0375	0.0302	0.0267	0.0249	0.0247	0.0249	0.0253
16	0.4659	0.1347	0.06	0.04	0.0322	0.0285	0.0265	0.0263	0.0266	0.027
17	0.485	0.1423	0.0635	0.0424	0.0341	0.0302	0.0281	0.0279	0.0282	0.0286
18	0.5033	0.1498	0.0671	0.0448	0.0361	0.0319	0.0297	0.0295	0.0298	0.0303
19	0.5209	0.1572	0.0706	0.0472	0.038	0.0337	0.0313	0.0311	0.0314	0.0319
20	0.5379	0.1645	0.0741	0.0496	0.04	0.0354	0.0329	0.0327	0.033	0.0335
21	0.5541	0.1717	0.0776	0.052	0.0419	0.0371	0.0345	0.0343	0.0346	0.0352
22	0.5698	0.1789	0.0811	0.0543	0.0438	0.0388	0.0361	0.0359	0.0362	0.0368
23	0.5848	0.1859	0.0845	0.0567	0.0458	0.0405	0.0377	0.0375	0.0378	0.0384

Note: Initial concentration of continuous phase is 1 at stage 24 and initial concentration of dispersed phase, $d_i = 0$, $i = 1, 2, 3, ..., 10$ at stage 0.

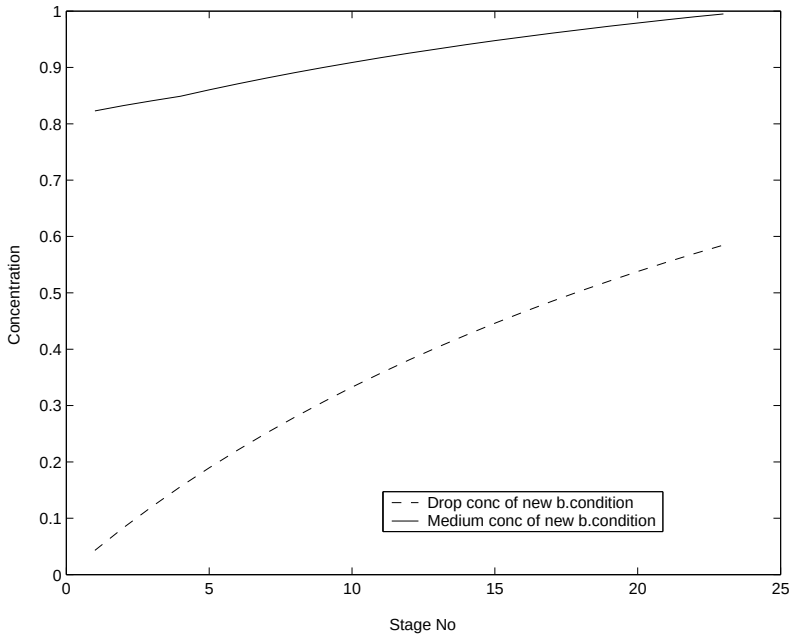

Figure 4.3: The profile of the medium and drop concentration along the column with respect to the new fractional approach to equilibrium

the continuous phase. In this mass transfer model, the process of solute transfer from continuous phase to the drops is described as follows.

We assume that initially the continuous phase has a unit concentration, that is in each stage j, for $j = 1, 2, 3, ..., n = 23$, the initial concentration of the continuous phase, $x(i_{itr}, j)$ is one where i_{itr} is the iteration number and j is the stage number. Then the first batch of drops with the same size is injected into the column. Each drop entering the first stage of the column has zero concentration.

This group of drops will move upward and break into smaller drops as they hit the first rotor disc. As in [4], the daughter drops are modelled as such that they are divided into ten different classes of size. It has to be noted that the mass transfer process in the real RDC column occurs simultaneously. Here we define the concentration of a certain group of drops with class size i, d_i in stage j as $y^{(i)}(i_{itr}, j)$. As these drops with initial concentration $y^i_{in}(i_{itr} = 1, j = 1)$ enter the first compartment, they are subjected to the medium concentration of the first compartment, $x_{in}(i_{itr}, j)$.

The drop surface concentration, $y^{(i)}_s(i_{itr} = 1, j = 1)$ in equilibrium with the continuous phase, $y^{(i)}_s(i_{itr} = 1, j = 1)$ at the interface is then obtained by Equations (4.15) and (4.16). In these equations, bulk concentration of the continuous phase, x_b is

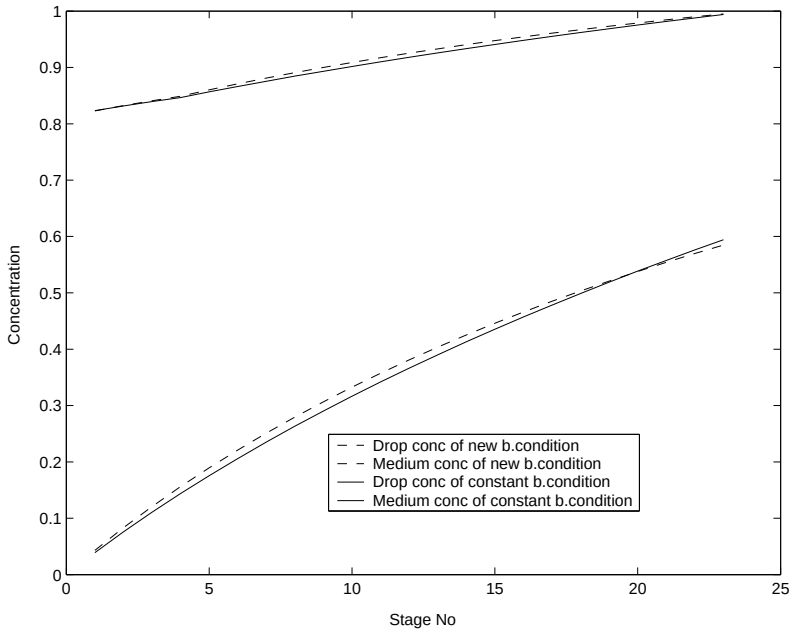

Figure 4.4: The profile of the medium and drop concentration along the column with respect to the new fractional approach to equilibrium and Crank solution

replaced by $x_{in}(i_{itr}, j) = 1$ and y_0 is replaced by $y_s^{(i)}(i_{itr} = 1, j = 1)$. After obtaining the drop surface concentration for each size, the next step is to determine the drop average concentration, $y_{av}^{(i)}(i_{itr}, j)$. This is obtained by using Equation (4.18). Then, the total concentration of the drops in each cell can be obtained from

$$y_{total}^{(i)} = N^{(i)}(j) \times V_{drop}^{(i)} \times y_{av}^{(i)}, \tag{4.20}$$

where $N^{(i)}(j)$ is the number of the drops in each cell i at stage j.

The next step is to calculate the average concentration of the drops in the first compartment by using

$$Y_{av} = \frac{\sum_{i=1}^{Ncl=23} N^{(i)} \times V_{drop}^{(i)} \times y_{av}^{(i)}}{\sum_{i=1}^{Ncl=23} N^{(i)} \times V_{drop}^{(i)}}. \tag{4.21}$$

The continuous phase concentration, $x_{out}(i_{itr}, j)$ after some amount of solute was transfered to the drops in the first compartment can be determined by using mass balance of Equation (4.19).

The process continues to the second stage. Before we start the process, the initial value of the drops and the medium have to be updated. The initial values of the drops at second stage are equal to $y_{in}^{(i)}(i_{itr} = 1, j = 2) = y_{av}^{(i)}(i_{itr} = 1, j = 1)$. Meanwhile at this time, the continuous phase concentration remains the same, $(x(i_{itr}, j) = 1)$.

After the updating process is completed, the process of mass transfer as explained above is repeated through the final stage.

Now, the process proceeds to the next iteration. Here, the updating process for the initial value of the drops and the continuous phase concentration also need to be done. At the second iteration the initial value of the drops is zero, whilst the continuous phase concentration, $x_{in}(i_{itr} = 2, j = 1) = x_{out}(i_{itr} = 1, j = 2)$. The mass transfer process is said to achieve the steady state if there exist $\epsilon = 0.0001$ such that $|y_{out}(i_{itr}, j) - y_{out}(i_{itr} - 1, j)| \leq \epsilon$.

The procedure to calculate the amount of mass transfer as explained in the above subsection is divided into two algorithms. The first is the Basic Mass Transfer Algorithm. In this algorithm, the amount of mass transfer from the continuous phase to the drops is calculated for given values of initial concentrations. The other is the main algorithm which is denoted as the Mass Transfer Multiple Drops Algorithm.

4.4.1 Basic Mass Transfer(BMT) Algorithm

This algorithm calculates the amount of mass transfer from the continuous phase to the drops.

Algorithm 4.2: Basic Mass Transfer(BMT) Algorithm

Input: x_{in} and $y_{in}^{(i)}$. **Output**: x_{out} and $y_{out}^{(i)}$.

Step 1: Read the input values. Calculate the value of the fractional approach to equilibrium based on the Varmulene equation, (4.6), the Crank equation, (3.26) and the new equation, (3.67) which is based on the varied boundary condition.

Step 2: Calculate the surface concentration of the medium and drops, $x_s^{(i)}$ and $y_s^{(i)}$, for $i = 1, 2, 3, ...10$ respectively by solving the non-linear equations of (4.15) and (4.16) using bi-section method. Set the bulk concentration of the medium, x_b is x_{in} and the initial drop concentration, y_0 is y_{in}.

Step 3: If $y_s^{(i)} > y_{in}^{(i)}$ for $i = 1, 2, 3, ...10$ go to Step 4, **else** set $y_{out}^{(i)} = y_{in}^{(i)}$, and go to Step 6.

Step 4: Determine the average concentration of the drops, $y_{av}^{(i)}$ for $i = 1, 2, 3, ...10$ using Equation (4.18).

Step 5a: Calculate the total concentration of the drops in each cell (i):

$$y_{total}^{(i)} = N^{(i)} \times V_{drop}^{(i)} \times y_{av}^{(i)}$$

where $N^{(i)}$ is the number of drops in each cell(i) at stage j.

Step 5b. Calculate the average concentration of the drops in jth stage using Equation (4.21).

Set $Y_{av} = y_{out}$ at stage j.

Step 6: Determine the concentration of the medium at jth stage by using the mass balance equation of (4.19).

Algorithm 4.2 is used in the Algorithm 4.3 to calculate x_{out} and $y_{out}^{(i)}$ at every stage.

4.4.2 Algorithm for the Mass Transfer Process of Multiple Drops in the RDC Column (MTMD Algorithm)

In the RDC column, the mass transfer process involved a swarm of drops. Therefore, to provide a more realistic mass transfer model in the RDC column, we will discuss the algorithm for the mass transfer process of the multiple drops as described in previous section. The mass transfer process is based on the drop distribution as explained in [4].

Algorithm 4.3: MTMD Algorithm

The algorithm calculates the amount of mass transfer from the continuous phase to the drops.

Step 1: Input all the geometrical details and physical properties of the system. Set $i_{itr} = 1$, $x_{in} = 1$ and $y_{in}^{(i)} = 0$, $\forall i = 1, 2, 3, ..., 10$.

Step 2: Initialize x_{in} and $y_{in}^{(i)}$, set $j = 1$.

Step 3: Apply BMT algorithm and calculate x_{out} and $y_{out}^{(i)}$. If $j > 23$ go to Step 5, **else** go to Step 4.

Step 4: Update the initial value for the next stage.

4a: If $i_{itr} = 1$ $\forall j = 1, 2, 3, ...n$ set $x_{in} = 1$, $y_{in}^{(i)} = y_{av}^{(i)}(i_{itr}, j)$

else go to 4b.

4b: If $(j <= n - 2)$ set $x_{in} = x_{out}(i_{itr} - 1, j + 2)$, $y_{in}^{(i)} = y_{av}^{(i)}(i_{itr}, j))$

else $(j = n - 1)$ $x_{in} = 1$, $y_{in}^{(i)} = y_{av}^{(i)}(i_{itr}, j)$

Set $j = j + 1$. Repeat Step 3.

Step 5: Set $\epsilon = 0.0001$. If $|y_{out}(i_{itr}, j) - y_{out}(i_{itr} - 1, j)| \leq \epsilon$, stop, **else** go to Step 6.

Step 6: Update the initial value for the next i_{itr}.

6a: Start with $i_{itr} = 1$ set $x_{in} = x_{out}(i_{itr}, j = 2)$, $y_{in}^{(i)} = 0$

6b: $i_{itr} = i_{itr} + 1$ set $x_{in} = x_{out}(i_{itr}, j = 2)$, $y_{in}^{(i)} = 0$ $\forall i_{itr} = 2, 3, 4, ...$

Set $i_{itr} = i_{itr} + 1$. Repeat Steps 2 to 5.

The algorithm is presented as a flow chart in Figure 4.5.

4.4.3 Simulation Results

The simulation of the mass transfer model based on MTMD Algorithm were carried out. For comparison purposes, the fractional approach to equilibrium based on the Crank solution is also used. To validate the algorithm, we use the experimental data from the SPS report (see Talib[4]). These data were produced by experimental work on the mass transfer process of an RDC column with the geometrical properties and system physical properties as given in Appendices A.1 and A.2. The results of the simulations can be found in Figure 4.6.

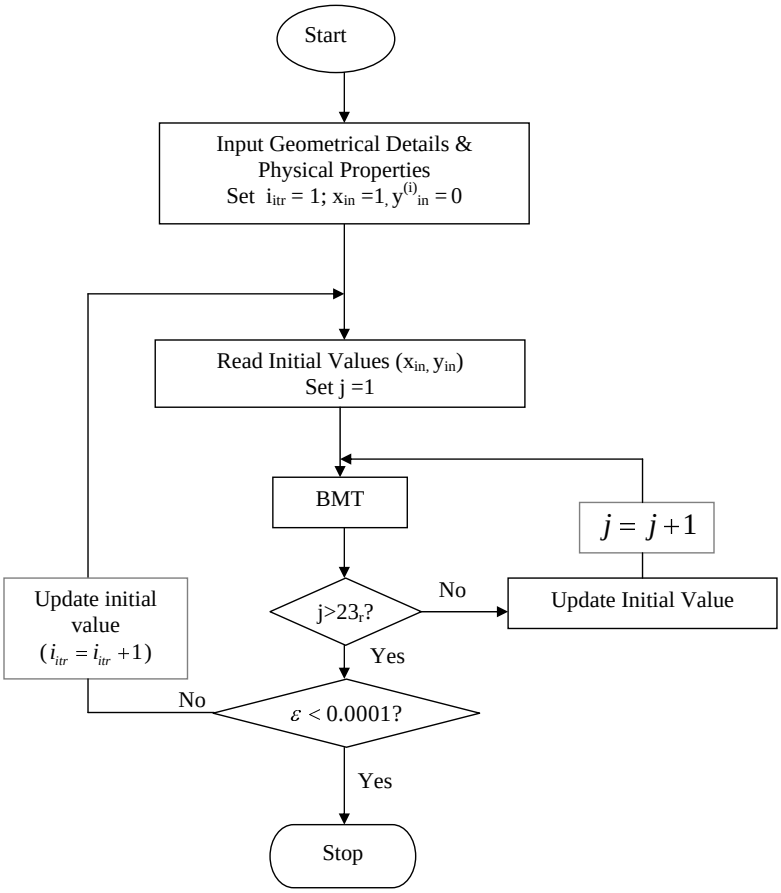

Figure 4.5: Flow chart for mass transfer process of MTMD Algorithm

Before the curve of the experimental data can be plotted (Figure 4.6), a few steps of normalization have to be considered. The first and second experimental data are given in Tables 4.2 and 4.3 respectively. Since the simulation of the forward modelling program uses normalized data, we need to find a technique to normalize the experimental data.

4.5 The Normalization Technique

To normalize the data, an equilibrium equation governing the mass transfer process of the system needs to be known. In this study, the system used is the iso-butyric acid/cumene/water system and the equilibrium equation of the system is

$$y_O = 0.135 x_A^{1.85}, \tag{4.22}$$

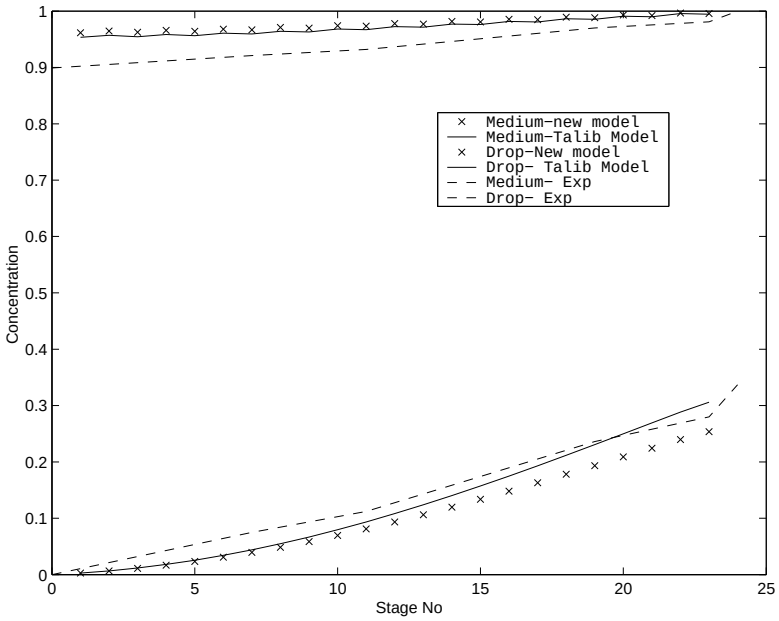

Figure 4.6: The concentration of continuous and dispersed phase of new model, Talib model and experimental

where y_O is the organic(cumene-drop) phase and x_A is the aqueous(continuous) phase, all measured in gram per litre(g/l).

The normalization technique used is explained in the following procedure:

4.5.1 Normalization Procedure

Procedure 1: (Normalization Procedure)

Step 1: Assume that x_{AF} is the feed concentration of continuous phase (iso-butyric acid in feed) and $y_{s_{max}}$ g/l is the iso-butyric acid in equilibrium with x_{AF}, the relation x_{AF} and $y_{s_{max}}$ is given by

$$y_{s_{max}} = 0.135 x_{AF}^{1.85}, \tag{4.23}$$

where y_O and x_A are replaced by $y_{s_{max}}$ and x_{AF} respectively.

Step 2: Dividing Equation (4.22) by (4.23), gives

$$y = x^{1.85} \tag{4.24}$$

Table 4.2: Experiment 1-Continuous phase (aqueous) and dispersed phase (organic) concentrations

Rotating disc contactor column with 152mm diameter and 23 stages

Mass transfer direction: continuous phase to drop phase

System : Cumene/Iso-butyric acid/Water

Rotor speed $N_R = 5rad/s$

Flow ratio (dispersed)/continuous phase) : 0.3333

Continuous phase (aqueous)	Dispersed phase (organic)
Flow rate: 3.75 l/m	Flow rate: 1.25 l/m
Feed concentration: 36.02 g/l	Feed concentration: 28.66 g/l
Exit concentration: 23.97 g/l	Exit concentration: 63.10 g/l

Stage	1	5	9	13	17	21
Continuous	24.02	24.95	26.18	27.85	30.10	32.91

Stage	3	7	11	15	19	23
Dispersed	-	36.34	40.08	46.46	52.80	57.33

where

$$y = \frac{y_O}{y_{s_{max}}}, \tag{4.25}$$

and

$$x = \frac{x_A}{x_{AF}}. \tag{4.26}$$

Step 3: Determine the normalized values of the dispersed phase concentration using Equation (4.25). In this study we assume that the feed concentration of the dispersed phase is zero. In order to satisfy this assumption, we use $y_O = y_{exp} - y_F$ where y_{exp} is the experimental value of dispersed phase concentration at particular stage and y_F is the feed concentration of the dispersed phase.

Step 4: Calculate the normalized values of the continuous phase concentration for each corresponding stage by mass balance equation, (4.19).

Table 4.3: Experiment 2-Continuous phase (aqueous) and dispersed phase (organic) concentrations

Rotor speed $N_R = 4.12 rad/s$

Flow ratio (dispersed)/continuous phase) : 0.3333

Continuous phase (aqueous)	Dispersed phase (organic)
Flow rate: 5.0 l/m	Flow rate: 1.67 l/m
Feed concentration: 39.64 g/l	Feed concentration: 27.28 g/l
Exit concentration: 25.12 g/l	Exit concentration: 60.98 g/l

Stage	1	5	9	13	17	21
Continuous	27.32	28.69	30.10	31.94	34.10	36.83

Stage	3	7	11	15	19	23
Dispersed	-	39.42	44.88	53.42	57.95	59.85

The detailed calculation for the normalized values of the dispersed and continuous phase are shown in the following example.

Example 1

In this example we use the experimental data 1 from Table 4.2.

Step 1: From Table 4.2, $x_{AF} = 36.02$, Substitute this into (4.23), we get $y_{s_{max}} = 102.3151$,

Step 2: Calculate the normalized value for dispersed concentration at stage zero (this stage corresponds to the feed) using Equation (4.25), that is $y_0 = \frac{28.66-28.66}{102.3151} = 0$.

Step 3: Repeat step 2 for stage 7,11,15,19,23 and 24, where stage 24 corresponds to the exit stage. At stage 7 we will get $y_7 = \frac{36.34-28.66}{102.3151} = 0.0751$.

Step 4: With the assumption that the feed concentration of the continuous phase is normalized so that its value is 1, Equation (4.19) is used to calculate the

normalized continuous phase for stage 0,7,11,15,19 and 23. In this case we have to calculate the normalized concentration at stage 23 first, that is $x_{23} = x_{24} - \frac{F_y}{F_x}(y_{24} - y_{23}) = 1.0 - 0.333(0.337 - 0.280) = 0.9810$. Repeat this step for stage 19, 15, 11, 7 and 0.

The results for all stages can be found in Table 4.4. The normalized process can also be done by first normalizing the continuous phase concentration followed by the dispersed phase which uses the mass balance equation. The same procedure is applied to the data in Table 4.3 which produced the normalized data in Table 4.4.

Due to the fact that the experimental data was not given for every stage, there was no data for the continuous concentration at stage 3, 7, 11,15, 19 and 23. In these circumstances, we have to construct a technique for de-normalization process to get the values of the concentrations in g/l at this stages.

Table 4.4: Experiment 1-Normalized continuous and dispersed phase concentrations

Stage	Continuous(x)	Dispersed(y)	Normalized x	Normalized y
0	23.97	28.66	0.899	0
1	24.02			
3		-		
5	24.95			
7		36.34	0.921	0.075
9	26.18			
11		40.08	0.932	0.112
13	27.85			
15		46.46	0.951	0.174
17	30.10			
19		52.80	0.970	0.236
21	32.91			
23		57.33	0.9810	0.280
24	36.02	63.10	1.0	0.337

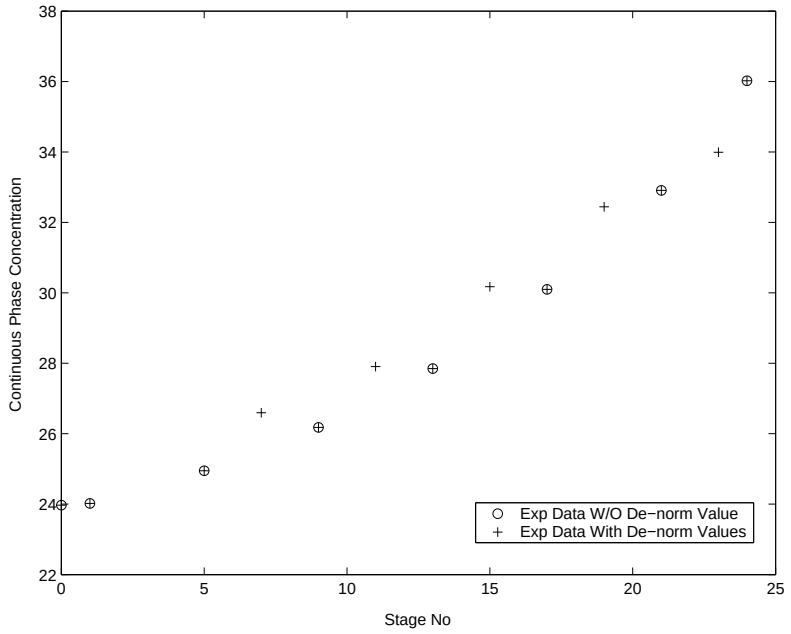

Figure 4.7: The continuous phase concentration along the column: Experiment Data 1

4.5.2 De-normalization Procedure

Procedure 2 (De-normalization Procedure)

Step 1: Assume that x_j and y_j are the normalized concentration of the continuous and dispersed phase respectively at stage i . X_j and Y_j are the experimental concentration value of the continuous and dispersed phase respectively. Assume also that the normalized concentration of the medium and its experimental value has a linear relationship, that is, its gradient is $m = \frac{X_{24}-X_0}{x_{24}-x_0}$.

Step 2: With the assumption that the normalized concentration of the medium and its experimental value has a linear relationship, calculate the experimental concentration of the medium of its respective normalized value:

$$X_j = X_{24} - m(1 - x_j). \tag{4.27}$$

For example at stage 0, $X_0 = X_{24} - m(1 - x_0)$.

Step 3: Repeat step 2 until all the approximated experimental values at the corresponding stage are calculated.

For the Data of Experiment 1, the de-normalization process will produce the approximated experimental data at corresponding stages as can be seen in Table 4.5. To

Table 4.5: Experiment 1-De-normalized continuous concentrations

Stage	Continuous(x)	Normalized x
0	**23.97**	0.899
1	24.02	
3		
5	24.95	
7	**26.5953**	0.921
9	26.18	
11	**27.9036**	0.932
13	27.85	
15	**30.1743**	0.951
17	30.10	
19	**32.441**	0.970
21	32.91	
23	**33.9919**	0.9810
24	**36.02**	1.0

see the effect of this de-normalization process on the experimental data, points with and without the de-normalization data are plotted against stage number. From the graph (see Figure 4.7), we can see that the trace of points containing de-normalized values at certain stage, oscillate about the trace of points of the actual experimental data. This phenomenon is explained by the fact that the de-normalized values at that particular stages are calculated from the normalized values which are calculated through Step 4 in Procedure 1. In other words, the normalized values are not directly calculated from the actual experimental values. Due to this reason there are some errors which affect the smoothness of the de-normalized data curve(trace of the points).

In this case we have to construct a better technique for the de-normalization process so that the de-normalized value curve will follow the behaviour of the actual experimental data curve. In order to do this we include the error factor in the de-normalization process, that is, in Step 2 of Procedure 2, Equation (4.27) becomes

$$X_j = X_{24} - m(1 - x_j) \pm \hat{e}, \tag{4.28}$$

where $\hat{e}$ is the error factor.

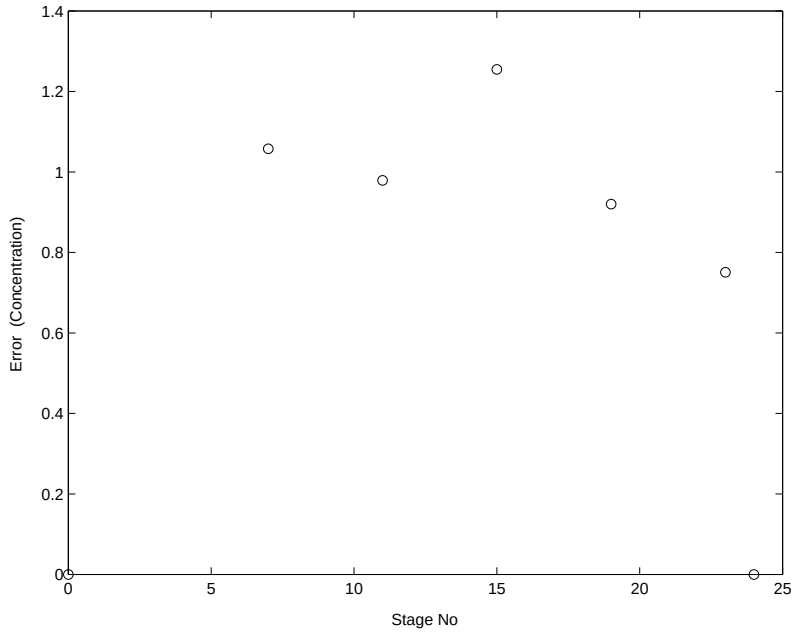

Figure 4.8: The error between the continuous phase concentration of Experiment Data 1 with and without de-normalized values

The differences between the two graphs in Figure 4.7 are then calculated along the column. The relationship between the differences and the stage number is then shown in Figure 4.8. It is then observed from Figure 4.8 that the error curve with respect to stage number of the column has quadratic-like curve. By using Matlab Basic Curve Fitting Tool-box, we represented the error data as a quadratic curve (see Figure 4.9) where the quadratic equation is

$$\hat{e}(j) = -0.0074j^2 + 0.1889j + 0.0001, \tag{4.29}$$

and j is the stage number of the column. This error function is then applied to Equation (4.28) which resulted in a corrected de-normalized continuous phase concentration data. These values are tabulated in Table 4.8. For comparison purposes, the corrected data is then plotted against stage number of the column in Figure 4.10.

In the next section, another algorithm for the mass transfer process of the multiple drops will be presented. In this model, the time when the next swarm of drops is injected into the column is taken into account.

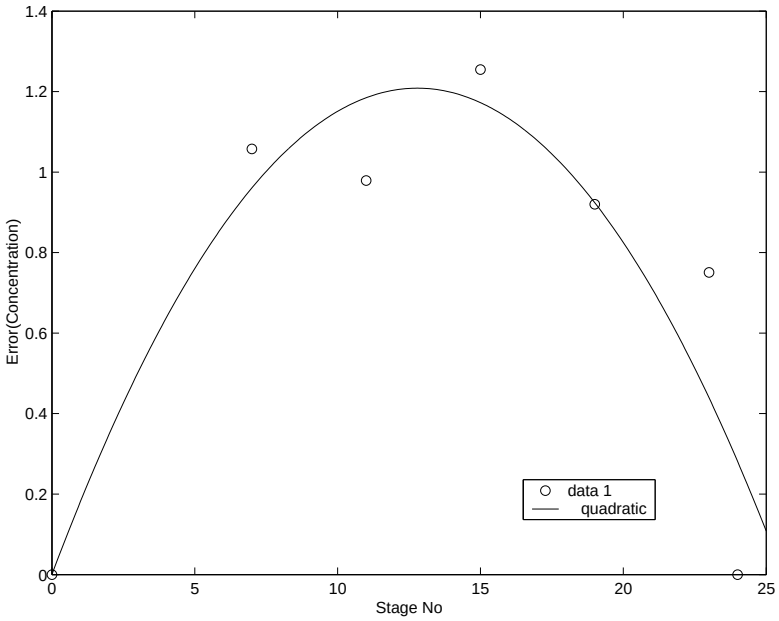

Figure 4.9: The error is fit to Quadratic-like curve

Table 4.6: The error by quadratic fitting

Stage	0	7	11	15	19	23	24
Error	0	0.9608	1.1848	1.1725	0.9240	0.4391	0

4.6 Forward Model Steady State Mass Transfer of Multiple Drops

In a real RDC column, the drops are continuously injected into the column according to the dispersed phase flow rate. This means that in order to produce the mass transfer model as close as possible to the real process, the time when the next swarm of drops is injected into the column need to be taken into consideration.

In this model, the mass transfer is calculated via the distribution of the drops which is assumed to be in a steady state. The model can be explained as follows. As in MTMD algorithm, we assumed that initially the continuous phase has a unit concentration, while the first batch of drops is injected into the column with zero concentration. This first swarm of drops with the same size will break into smaller drops as they hit the first rotor disc.

These daughter drops are distributed into the cells according to their sizes as explained in Section 4.4 . At the same time the mass transfer process occurs. The

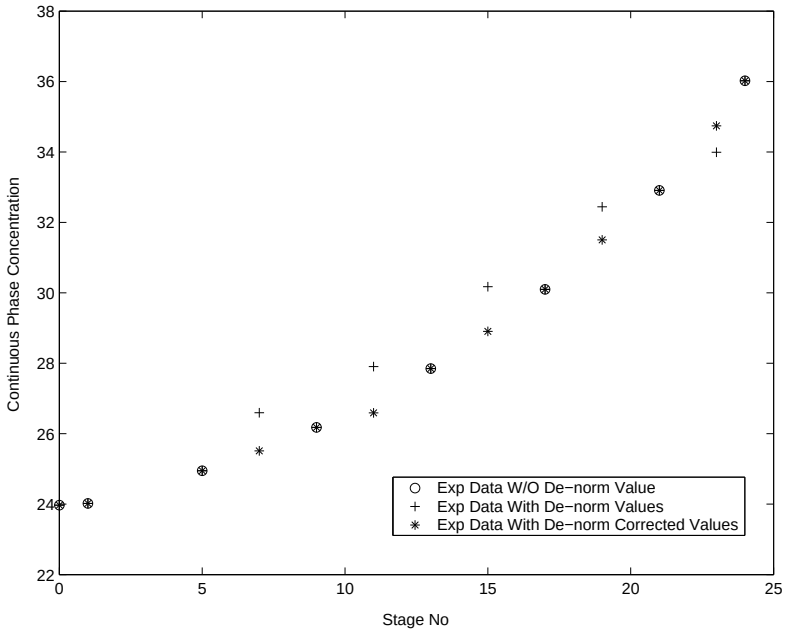

Figure 4.10: The continuous phase concentration along the column with corrected value : Experiment Data 1

equations used are exactly the same as in MTMD algorithm. The steps of calculation can easily be understood if we refer to the flow chart in Figure 4.11.

In the following algorithm, when the second swam of drops is injected into the column, the drops will also move upward and break into smaller drops as they hit the first rotor disc (in this algorithm we assumed that the number of iteration is equal to the number of batches of drops injected into the column). Now, the second batch will fill the first compartment whilst the first one moves to the second compartment. The steps for calculating the mass transfer of the drops in the first compartment are exactly the same as the first batch of the drops.

However, for the second compartment, we take the initial concentration of the drops, y_{in} as the output concentration of the drops when the iteration is equal to one, that is $y_{in}(i_{itr} = 2, j = 2) = y_{out}(i_{itr} = 1, j = 1)$. At this time the initial concentration of the continuous phase remains the same, $x_{in} = 1$. The complete procedure for calculating the mass transfer at this stage is shown in Figure 4.12.

Now, when the third swam of drops enter the column, the same phenomenon will occur, but this time the initial concentration of the continuous phase at the first compartment is subjected to the output concentration of the continuous phase at the

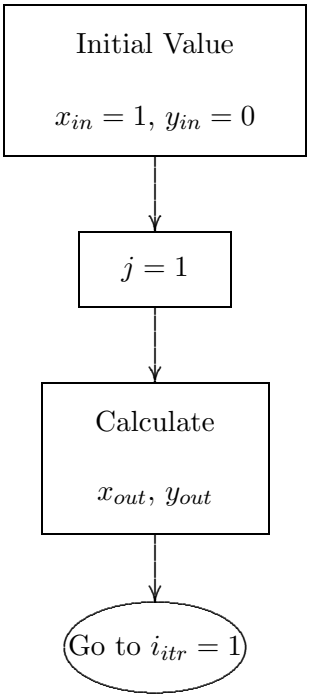

Figure 4.11: Flow chart for mass transfer process at $i_{itr} = 1$

second compartment when the iteration is equal to two, that is $x_{in}(i_{itr} = 3, j = 1) = x_{out}(i_{itr} = 2, j = 2)$. Meanwhile the initial concentration of the drops, $y_{in}(i_{itr} = 3, j = 1) = 0$. The initial concentrations for the mass transfer at the second and third compartments can be determined by following the steps given in the flow chart in Figure 4.13.

The same steps apply to the $4th, 5th, 6th, ..., nth$ swarm of drops. The step that explains the way to determine the initial concentrations at particular stage is shown in Figure 4.14. The phenomenon explained above will continue until the first batch or group reaches the 23rd compartment (stage). At this instance the column is full of drops. The iteration will continue until the concentration of the drops is in steady state. In other words, the difference of the concentration for both phases at time t and $t - 1$ is very small or negligible. The schematic diagram in Figure 4.15 illustrates the phenomenon explained above.

The steps to calculate the amount of mass transfer as explained in this section is divided into three algorithms. The first one is the Basic Mass Transfer Algorithm.

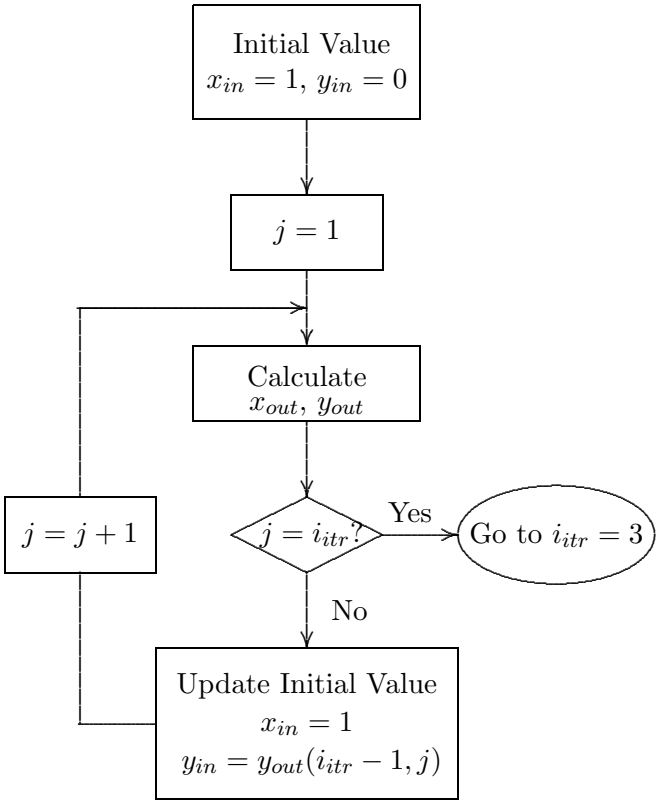

Figure 4.12: Flow chart for mass transfer process at $i_{itr} = 2$

In this algorithm, the amount of mass transfer from the continuous phase to the drops is calculated for given values of initial concentrations. The next subsection is the main algorithm which is denoted as the Mass Transfer Steady State Algorithm. It is then followed by the Updating Mechanism Algorithm which is divided into two, these are the Updating Initial Value for Next Iteration and the Next Stage Algorithms.

4.6.1 Algorithm 4.4: Algorithm To Find The Drop Concentration of a Steady State Distribution in 23 Stages RDC Column (MTSS Algorithm)

The algorithm calculates the amount of the mass transfer from the continuous phase to the drops.

Step 1: Input all the geometrical details and physical properties of the system. Set

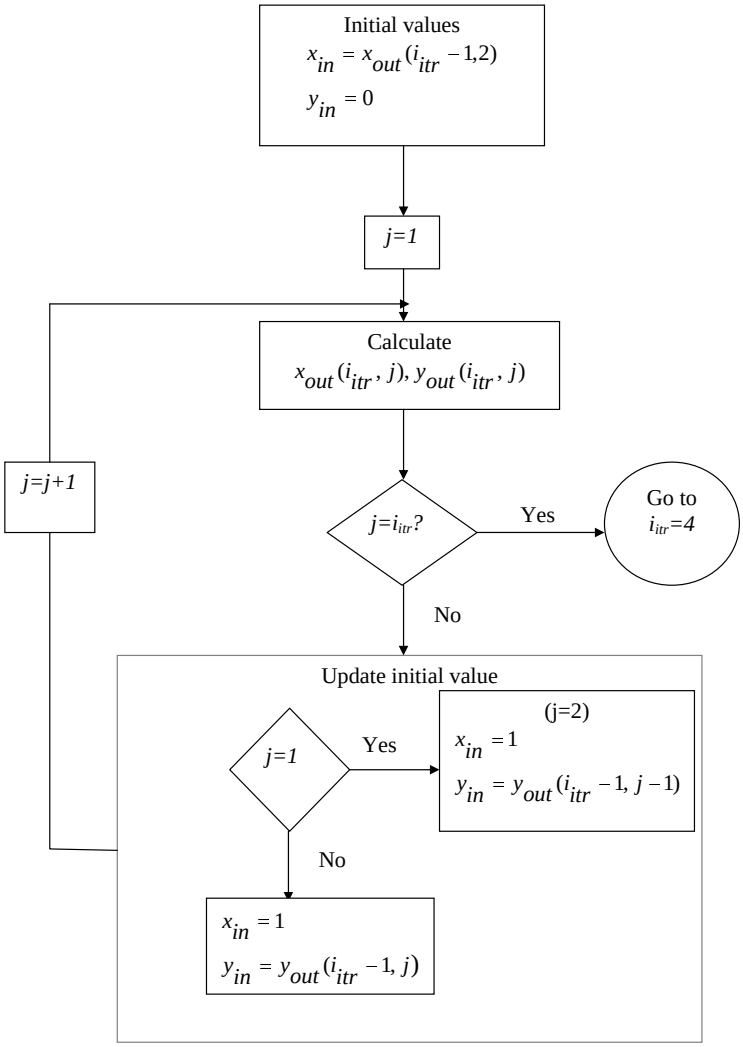

Figure 4.13: Flow chart for the mass transfer process at $i_{itr} = 3$

$i_{itr} = 1$, $x_{in} = 1$ and $y_{in}^{(i)} = 0$, $\forall i = 1, 2, 3, ..., 10$.

Step 2: Read initial values, that is x_{in} and $y_{in}^{(i)}$, set $j = 1$.

Step 3: If $i_{itr} \leq n$, go to step 4, **else** go to Step 7.

Step 4: Apply BMT algorithm to calculate x_{out} and $y_{out}^{(i)}$.

Step 5: If $j < i_{itr}$, go to Step 6, **else update** initial value for $i_{itr} = i_{itr} + 1$ go to Step 3,

Step 6: **Update** the initial value for the next stage. Set $j = j + 1$, repeat Steps 4 to 5.

Step 7: Now $i_{itr} = n + 1$. Read the input values and set $j = 1$.

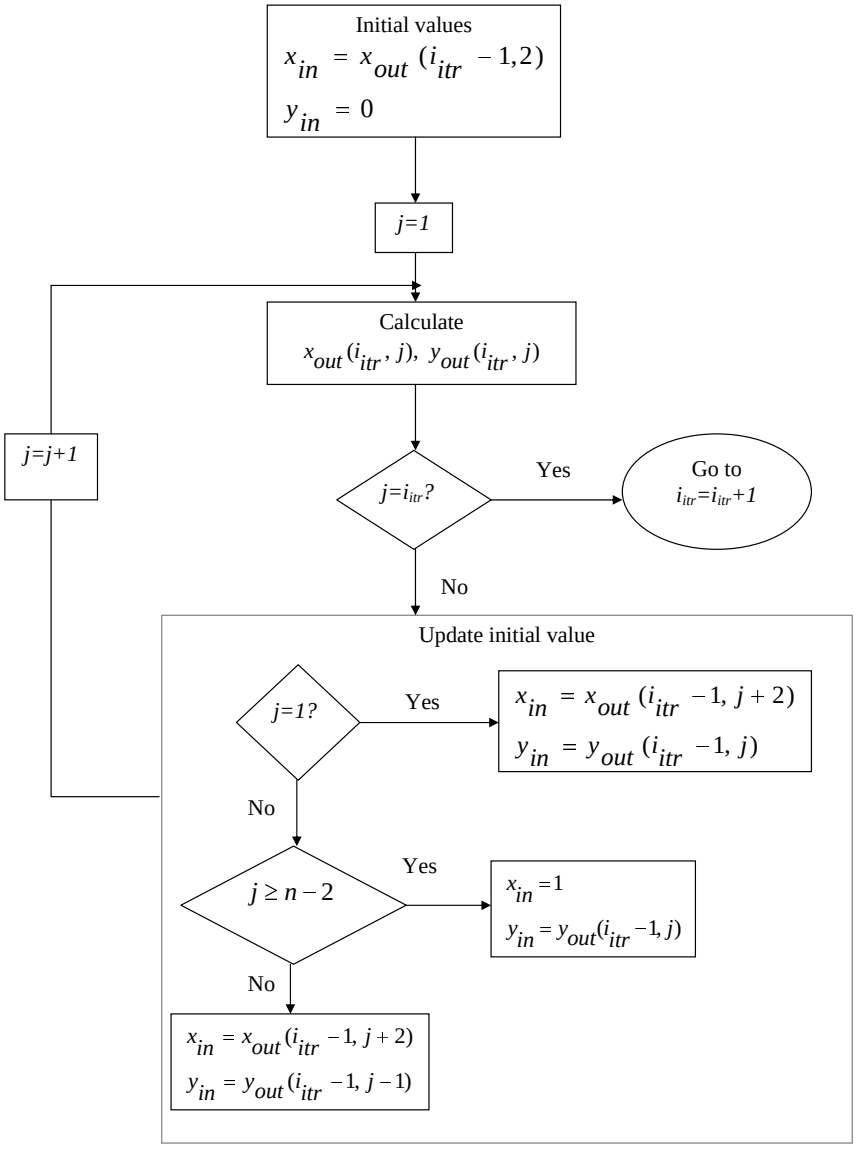

Figure 4.14: Flow chart describing the mass transfer process for $i_{itr} = 4, 56, ..., n$

Step 8: Apply BMT algorithm to calculate x_{out} and $y_{out}^{(i)}$.

Step 9: If $j < n$. **Update** the initial values for the next stage. Set $j = j + 1$, repeat Steps 8 to 9, **else** go to Step 10.

Step 10: Set $\epsilon = 0.0001$. If $|y_{out}(i_{itr}, j) - y_{out}(i_{itr} - 1, j)| \leq \epsilon$, stop, **else Update** the initial value for the next i_{itr}. Set $i_{itr} = i_{itr} + 1$, repeat Steps 8 to 9.

To update the initial value for the next stage and for the next iteration, the following algorithms are considered.

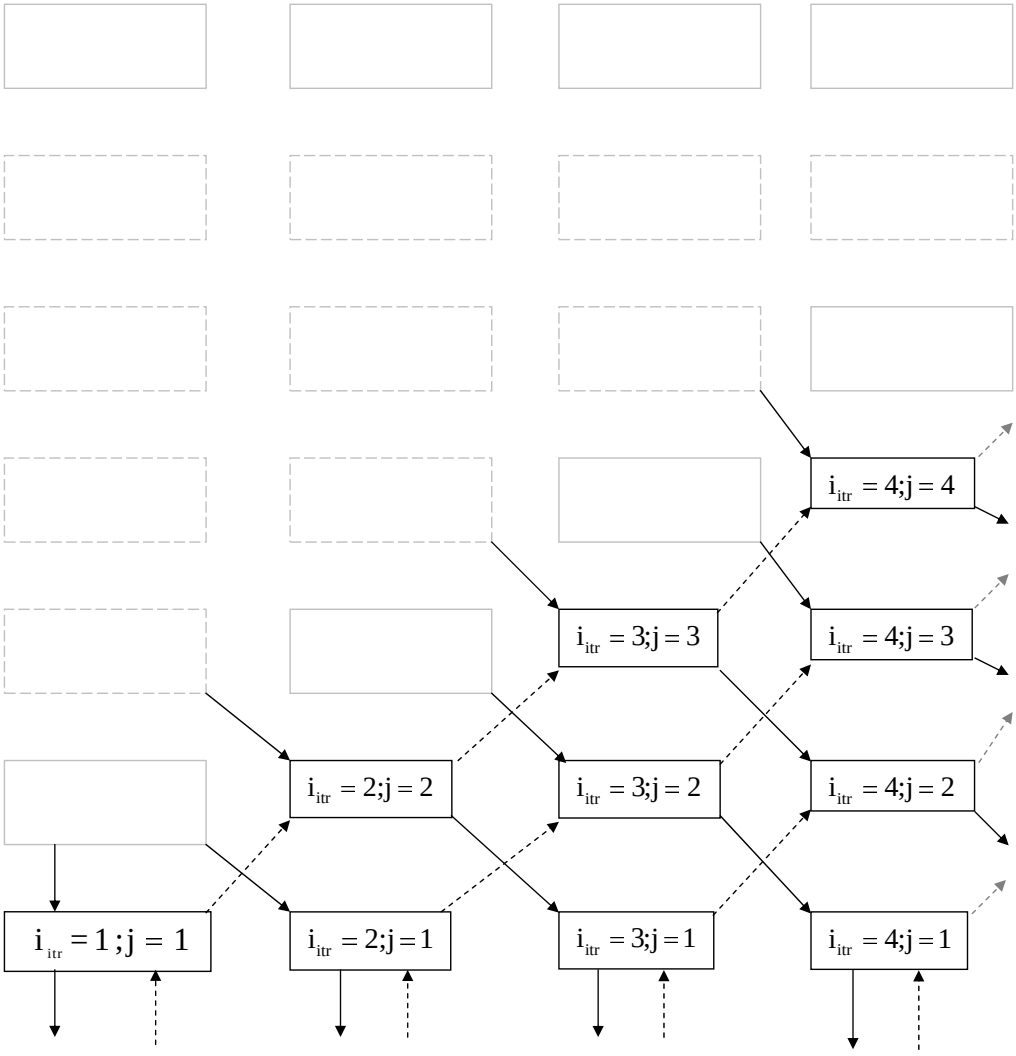

Figure 4.15: Schematic diagram of the mass transfer process in the 23-stage RDC column

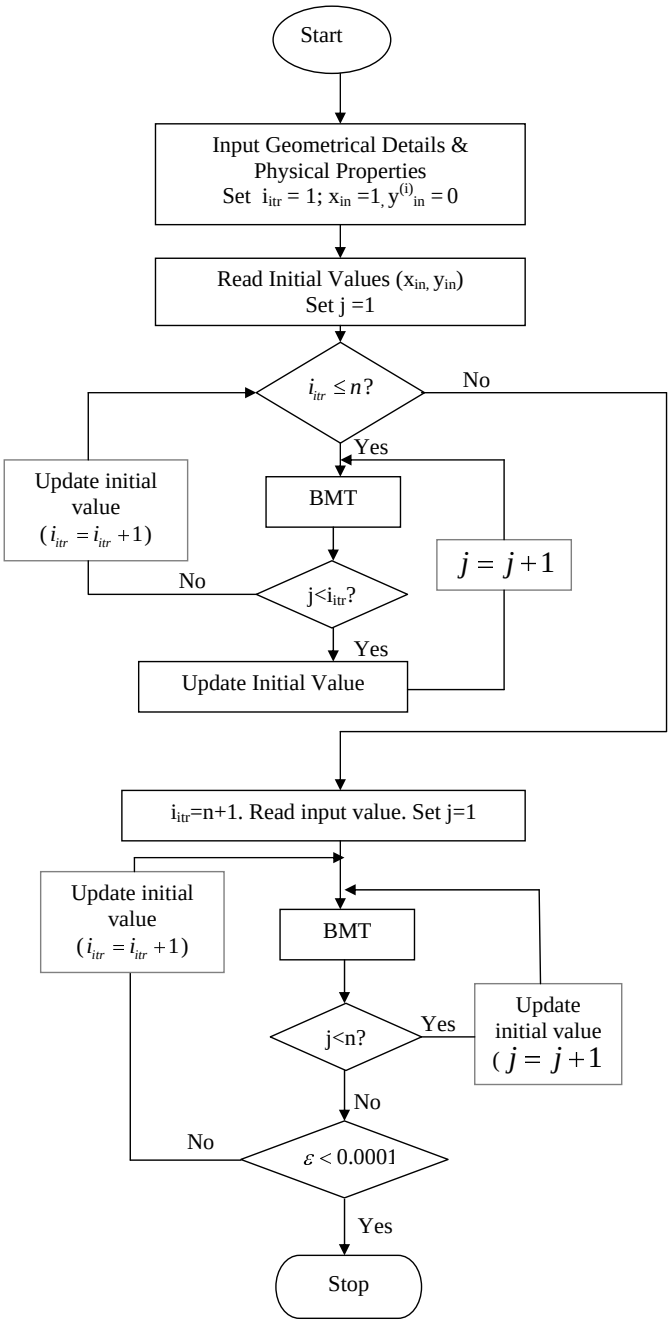

Figure 4.16: Flow chart for mass transfer process of MTSS Algorithm

4.6.2 Updating Mechanism Algorithm

Algorithm 4.5: Updating the Initial Value for Next Iteration (i_{itr}) (UIVI) Algorithm

The Algorithm is used to update the initial values for the next iteration.

Step 1 Read the current position of i_{itr} and j.

Step 2 If $i_{itr} = 1$, the updating input values of next iteration is $x_{in} = 1$, $y_{in}^{(i)} = 0$

else $(i_{itr} > 1)$, the updating input values of next iteration is $x_{in} = x_{out}(i_{itr} - 1, 2)$, $y_{in}^{(i)} = 0$

Algorithm 4.5: Updating the Initial Value for the Next Stage (j) (UIVS) Algorithm

The Algorithm is used to update the initial values for the next stage (j)

Step 1: Read the current position of i_{itr} and j.

Step 2: If $i_{itr} \leq n$ go to Step 3 **else** go to Step 5.

Step 3: If $j < i_{itr}$

if $(1 < i_{itr} \leq 3) \Rightarrow x_{in} = 1$, $y_{in}^{(i)} = y_{av}^{(i)}(i_{itr} - 1, j)$

else$(4 \leq i_{itr} \leq n)$

if $(j = 1) \Rightarrow x_{in} = x_{out}(i_{itr} - 1, j + 2)$, $y_{in}^{(i)} = 0$

elseif $j \geq i_{itr} - 2 \Rightarrow x_{in} = 1$, $y_{in}^{(i)} = y_{av}^{(i)}(i_{itr} - 1, j)$

else $(2 \leq j < i_{itr} - 2) \Rightarrow x_{in} = x_{out}(i_{itr} - 1, j + 2)$, $y_{in}^{(i)} = y_{av}^{(i)}(i_{itr} - 1, j)$

else $(j < i_{itr})$ go to Step 4

Step 4: Apply the UIVI Algorithm to update the initial values for the next iteration.

Step 5: $(i_{itr} > n)$

If $j = 1 \Rightarrow x_{in} = x_{out}(i_{itr} - 1, j + 2)$, $y_{in}^{(i)} = 0$

elseif $j \geq n-2 \Rightarrow x_{in} = 1$ $y_{in}^{(i)} = y_{av}^{(i)}(i_{itr}-1, j)$

else$(2 \leq j < n-2) \Rightarrow x_{in} = x_{out}(i_{itr}-1, j+2)$, $y_{in}^{(i)} = y_{av}^{(i)}(i_{itr}-1, j)$.

4.6.3 Simulation Results

The simulations of the mass transfer model based on the MTSS Algorithm were carried out. For comparison purposes, the output concentrations of the continuous and dispersed phase for both MTSS and MTMD algorithms are listed in Table 4.7. To analyze the result graphically, the six curves from MTSS, MTMD and experimental data are plotted in Figure 4.17.

4.7 Discussion and Conclusion

A detailed description of the development of the mass transfer models has been presented in this chapter. It begins with the concept of the diffusion equation which is based on the interface concentration. In these models, the new fractional approach to equilibrium was used to get the flux across the drop surface of Equation (4.10). From this derivation, the term referred to *Time Dependent Quadratic Driving Force* was formulated.

The MTASD Algorithm was designed based on the concept explained above. This algorithm calculates the amount of solute transfer from the continuous phase to a single drop. The simulations of the algorithm were also carried out for different size of drops. The range of the size is from 0.0004 to 0.0007 meter in diameter. The output concentrations of the drops for each size were listed in Table 4.1. From the data, it can be seen that, the concentration of a smaller drop is higher than the bigger one at every stage. This is because the smaller drop provides larger surface area compared to the other. In fact, the velocity of the smaller drop is less, meaning that the smaller drop has a higher residence time in each compartment.

Besides the new fractional approach to equilibrium, we also run the MTASD algorithm using the fractional approach to equilibrium based on the Crank solution.

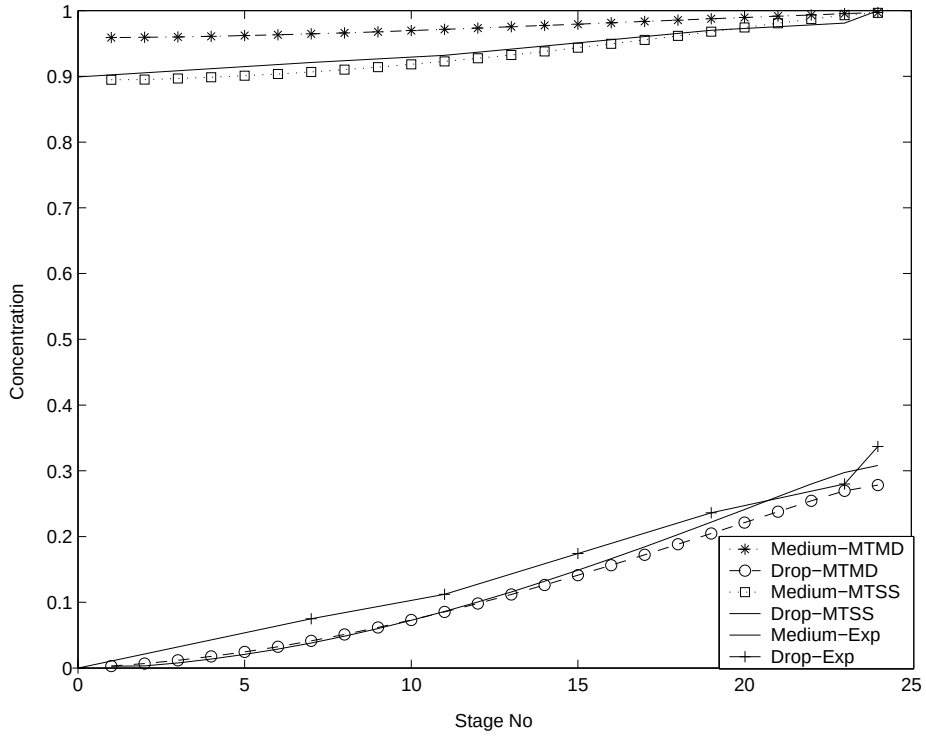

Figure 4.17: The concentration of continuous and dispersed phase of MTMD, MTSS Algorithm and Experimental

The simulation data of the medium and drop concentrations were plotted in Figure 4.4. The profile of the curve using the new fractional approach to equilibrium agrees with the one based on the Crank solution.

The idea to provide a model which is close to the real process of the mass transfer in the column has driven us to develop the MTMD algorithm. This algorithm calculates the mass transfer of the multiple drops. The drop distribution as explained in Talib[4] was considered. To validate the algorithm, we used the experimental data in Tables 4.2 and 4.3. These data have to be normalized, before the comparison of the data could be made. Figure 4.6 shows six curves of the continuous and dispersed phase concentrations for the mass transfer model developed by Talib, the new model of MTMD algorithm and from the experimental data.

Although the result of MTMD algorithm showed that the model agrees with the profile of the experimental data, in Section 4.6 another algorithm named MTSS algorithm for the multiple drops mass transfer process was presented. In MTMD algorithm the calculation of the mass transfer for the first batch of the drops was

carried out up to the final stage without considering when the second batch of drops was injected into the column. It seems that, in this algorithm the second batch of drops was only injected when the first batch reached the top of the column. Similarly, the third batch of drops would be injected when the calculation of mass transfer for the second batch had been completed for all stages.

On the other hand, we considered the time when the next swarm of drops was injected in MTSS algorithm. In this work, we assumed that the flow rate of the dispersed phase was equal to the simulation time for each iteration. Therefore, in the MTSS algorithm, the mass transfer for the second batch of the drops would be calculated even as the first one just reached the second compartment. The process of construction of the algorithm was illustrated in flow charts of Figures 4.11, 4.12, 4.13 and 4.14. The output concentrations for the continuous and dispersed phase from MTSS and MTMD were listed in Table 4.7. From these data, we conclude that the outputs from both algorithms do not give much difference. Figure 4.17 clearly is in agreement with the above conclusion.

However, MTSS Algorithm has close trait to the real phenomenon of the mass transfer process in the RDC column. It is because in the real RDC column the mass transfer occurs simultaneously as explained in the MTSS Algorithm. Therefore, we conclude that MTSS Algorithm gives a better representation of the real mass transfer process and hence it is expected to produce better simulation results when compared to the experimental data. The latter conclusion is in accordance with the dispersed and continuous phase concentrations curves as shown in Figure 4.17.

The MTASD, MTMD and MTSS algorithms described in this chapter can be used successfully to calculate the amount of mass transfer from the continuous phase to dispersed phase.

Table 4.7: The concentration of the dispersed and continuous phase according MTMD and MTSS Algorithm

Stage No	Continuous (MTMD)	Dispersed (MTMD)	Continuous (MTSS)	Dispersed (MTSS)
1	0.959	0.003	0.8949	0.0027
2	0.9594	0.0068	0.8951	0.0033
3	0.96	0.0117	0.8966	0.0078
4	0.9608	0.0176	0.8985	0.0136
5	0.9619	0.0245	0.9009	0.0206
6	0.9631	0.0324	0.9036	0.0287
7	0.9645	0.0412	0.9067	0.038
8	0.966	0.051	0.9102	0.0485
9	0.9678	0.0616	0.914	0.06
10	0.9695	0.073	0.9181	0.0725
11	0.9715	0.0853	0.9226	0.086
12	0.9733	0.0982	0.9275	0.1005
13	0.9754	0.1119	0.9325	0.1157
14	0.9773	0.1262	0.9379	0.1319
15	0.9794	0.1411	0.9436	0.1488
16	0.9814	0.1564	0.9494	0.1663
17	0.9835	0.1722	0.9554	0.1843
18	0.9855	0.1883	0.9616	0.203
19	0.9875	0.2047	0.9679	0.2219
20	0.9895	0.2212	0.9743	0.241
21	0.9915	0.2378	0.9808	0.2606
22	0.9933	0.2544	0.9872	0.2799
23	0.9953	0.2694	0.993	0.2974
24	0.9971	0.2783	0.9966	0.3081

CHAPTER 5

CONCLUSIONS AND FURTHER RESEARCH

5.1 Introduction

This chapter provides a summary and an overall conclusion of the findings presented in this work and also gives an outline of some further research which are worthwhile investigating in the future.

5.2 Summary of the Findings and Conclusion

The initial task of the work was to formulate an equation that will be used as the boundary condition of the IBVP. This equation was expected to be a time varying function. This was achieved by using the experimental data from [4]. From the data, it was found that the concentration of the continuous phase depends on the stage of the RDC column. In this work, the following assumptions are adopted:

- there are ten different classes of drops with different velocities depending on their sizes,
- mass transfer of a single solute from continuous phase to a single drop,
- the drop is spherical and there is no coalescence of drops,
- the concentration of the drop along the radius r is assumed to be uniform

- drop contact time for mass transfer coefficient estimation is residence time in the compartment.

With these assumptions and by the least square method, it was found that the boundary condition is a function of t, that is $f_1(t) = a_1 + b_1 t$. The analytical solution of the IBVP with the new boundary condition was detailed in Subsection 3.3.1.

The derivation of the new fractional approach to equilibrium was then considered based on the analytical solution of the varied boundary condition IBVP. The comparison of the new and existing fractional approach to equilibrium was carried out by plotting the curves with respect to time on the same axes as in Figure 3.3. The curve of the new fractional approach to equilibrium profile agrees with the result obtained by Talib[4]. Therefore, from this initial task we conclude that the new fractional approach to equilibrium, F_{new}, represents the real phenomena of the mass transfer and hence gives better tool for further development of the improved mass transfer model in the column.

The development of the improved mass transfer model is one of the main aims in this research. Therefore the IBVP which is based on the interface concentration was considered. With this consideration and the new fractional approach to equilibrium, a new driving force named Time-dependent Quadratic Driving Force (TQDF), $(\frac{(f_1(t)-c_1)^2-(C_{av}-c_1)^2}{C_{av}-c_1})$, was derived. The process of mass transfer of a single drop based on TQDF is governed by:

1. The equilibrium equations

   $y_s = f(x_s)$,

2. The interface equation

   $y_s = \frac{3d}{D\pi^2} k_x (x_b - x_s) \frac{F_v}{1-F_v^2} - (\frac{3d}{D_y \pi^2})(\frac{F_v}{1-F_v^2})(\frac{d}{6}) F_v(t) \frac{1}{dt} f_1(t) + y_0$,

3. The average concentration of the drop

   $y_{av} = F_{new}(t)(y_s - y_0) + y_0$,

4. The mass balance equation

   $F_x(x_{in} - x_{out}) = F_y(y_{out} - y_{in})$.

Based on these equations, the MTASD Algorithm was designed. This algorithm calculates the amount of mass of a solute transfer from the continuous phase to a single drop in the column. The process of mass transfer is said to be in a steady state, if there exist $\varepsilon = 0.0001$ where the difference of the concentration at $t = n$ and $t = n - 1$ is less or equal to ε at every stage. At this point, the concentration of the drop interface is in equilibrium with the medium. The complete description of the algorithm is well illustrated as a flow chart in Figure 4.2.

The simulation of the MTASD Algorithm was also carried out using the Crank solution of fractional approach to equilibrium, F_c. The validation of the MTASD Algorithm was done empirically by plotting the curves of the simulation results from both F_{new} and F_c. It was found from Figure 4.3 that the curves of the dispersed and continuous phase concentrations from the improved model agree with the curves from the existing model in [4].

Based on various studies, the mass transfer process in the RDC column is very complicated because it involves not only the mass transfer of a single drop but infinitely many drops. These drops have different sizes and different velocities. Therefore, a more realistic MTMD Algorithm is constructed which was later refined as another algorithm, MTSS Algorithm. Both of the algorithms calculate the mass transfer of multiple drops in 23-stages RDC column.

In this model, the total concentration of the drops in each cell is obtained by applying Equation (4.20). Then using Equation (4.21), the average concentration of the drop in each compartments is calculated. Finally the mass balance equation is applied in order to obtain the amount of solute transfer from the continuous to the dispersed phase. In the MTSS Algorithm the calculation of the mass transfer was done simultaneously with respect to iteration time. In other word, as an example, the mass transfer for $i_{itr} = 2$ is calculated at stage two for the first swam of drops and at stage one for the second swam of drops. This is contrary to MTMD Algorithm. In the MTMD algorithm, the mass transfer at $i_{itr} = 1$ is calculated at every stage without considering the second swam of drops. The simulation data of both algorithms and the experimental data are then plotted in Figure 4.17.

From this figure, it was empirically found that the output from both algorithms do not give significant difference. However, MTSS Algorithm is more realistic due to

the fact that mass transfer in the real RDC column occurs simultaneously as explained in the MTSS Algorithm. In conclusion, MTSS Algorithm gives a better representation of the real mass transfer process and hence it is expected to produce better simulation results when compared to experimental data. The dispersed and continuous phase concentrations curves in Figure 4.17 clearly show the agreement of the above conclusion.

For more definitive conclusion, the improved mass transfer model, where by the output can be simulated MTSS Algorithm, gives a useful information and provides better simulation results and hence better control system for the RDC column.

5.3 Further Research

This research presents the improved mathematical forward mass transfer model for simulation of RDC Column. All the objectives of the research are achieved successfully. However, the following research suggestions, in our opinion are worthwhile investigations:

- Establishment of a technique for assessing the inverse models of the corresponding new forward mass transfer models.

  The MTASD, MTMD MTSS algorithms described in this report can be used successfully to calculate the amount of mass transfer from continuous phase to dispersed phase. But this type of modelling, which is known as forward modelling is not efficient enough to determine the required input parameters in order to produce certain values of output parameters. The determination of the input values by trial and error consumes a lot of computer time and it will be costly if actual processes were involved. Therefore, a new technique which is based on fuzzy approach is suggested in a further research to determine the input concentration of both phases for a certain value of output concentrations. This type of modelling is called inverse modelling.

- Development of Inverse Model of the hydrodynamic process.

  The parameters involved in the hydrodynamic process in the RDC column are complexly interrelated. Therefore only certain parameter values can be

controlled and adjusted such as that of rotor speed (N_r), dispersed phase flow rate (F_d) and interfacial tension (γ). Although interfacial tension could not be controlled directly but at least by varying this value will provide us with some useful information. These three parameters are determined or fixed outside the RDC column, but once they are applied to the modelling, it will give whatever calculated value for the holdup. This is an inverse problem of type *coefficient inverse problem*.

- Development of the intra-stage control system for the RDC column.

  In this study the inverse problem in determining the value of the input parameter for the desired value of output of 23-stage RDC column has been successfully solved. Intra-stage control system is the control system inside the RDC column. The inverse algorithm developed in this study only need the information of the input and output parameters outside the RDC column. Whilst for the intra-stage control, more information is needed in particular the information on the concentrations of both liquids at certain stage or if possible at every stage in the RDC column.

- Further investigation and development on the theory of two dimensional fuzzy number in multi-stage systems.

- Development of the integrated model of the hydrodynamic and mass transfer processes.

  Parallel processing is suggested to be introduced in order to develop the integrated model of the hydrodynamic and mass transfer processes. This integrated model is hoped to give better simulation and better control system for the RDC column.

REFERENCES

1. Warren, L.M. *Unit Operations of Chemical Engineering.* Sixth Edition. Singapore: McGraw-Hill Higher Education 2001

2. Kertes, A.S. The Chemistry of Solvent Extraction. In: Hanson, C. *Recent Advances in Liquid-liquid Extraction.* Exeter, Great Britain: Pergamon Press. 15-92; 1975

3. Korchinsky, W.J. and Azimzadeh, An Improved Stagewise Model of Countercurrent Flow Liquid-liquid Contactor *Chemical Engineering Science.* 1976. 31(10): 871-875

4. Talib, J. *Mathematical Model of Rotating Disc Contactor Column.* Ph.D. Thesis. Bradford University, Bradford, U.K.; 1994

5. Ghalehchian, J. S. *Evaluation of Liquid-Liquid Extraction Column Performance for Two Chemical System*, Ph.D. Thesis. Bradford University, Bradford, U.K.; 1996

6. Arshad, K.A. *Parameter Analysis For Liquid-Liquid Extraction Coloumn Design.* Ph.D. Thesis, Bradford University, Bradford, U.K.; 2000

7. Crank, J. *The Mathematics of Diffusion.* Second Edition. London: Oxford University Press. 1978

8. Lo, T.C. and Malcolm, H.I.B. *Extraction Liquid-Liquid.* Kirk-Othmer Encyclopedia of Chemical Technology 4th Ed. vol 10, John Wiley & Sons 1994.

9. Blumberg, R., Gonen, D. and Meyer, D. Industrial Inorganic Processes. In: Hanson, C. *Recent Advances in Liquid-liquid Extraction.* Exeter, Great Britain: Pergamon Press. 93-112; 1975

10. Coleby, J. and Graesser R. Industrial Organic Processes. In: Hanson, C. *Recent Advances in Liquid-liquid Extraction.* Exeter, Great Britain: Pergamon Press. 113-138; 1975

11. University of Bradford and The Institution of Chemical Engineers. *Introduction to Solvent Extraction Technology.* Bradford. 1975

12. School of Chemical Engineering, University of Bradford and British Nuclear Fuel Plc. *Chemical Engineering: An Introductory Awareness Course.* Bradford. 1987

13. Laddha, G.S. and Degaleesan, T.E. *Transport Phenomena in Liquid Extraction.* Tata Mc.Graw-Hill Publishing Co Ltd. 1976

14. Koster, W.C.G. *Handbook of Solvent Extraction.* J. Wiley and Sons. 1983

15. Reissinger, K.H. and Schroter J. Selection Criteria for Liquid-liquid Extractor. *Chemical Engineering.* 1978. 85:109-118.

16. Korchinsky, W.J. Rotating Disc Contactor. In: Godfrey, J.C. and Slater, M.J. *Liquid-Liquid Extraction Equipment.* England: J. Wiley and Sons. 247-276; 1994

17. Gourdan, C., Casamatta, G. and Muratet, G. Population Balance Based Modelling. In: Godfrey, J.C. and Slater, M.J. *Liquid-Liquid Extraction Equipment.* England: J. Wiley and Sons. 137-226; 1994

18. Godfrey J.C. and Slater, M. J. Slip Velocity Relationships for Liquid-liquid Extraction Columns. *Transaction Industrial Chemical Engineers* 1991. 69:130-141

19. Weiss, J., Steiner L. and Hartland S. Determination of Actual Drop Velocities in Agitated Extraction Column*Chemical Eng. Science.* 1995. 50(2):255-261

20. Bahmanyar, H. *Drop Breakage and Mass Transfer Phenomena in a Rotating Disc Contactor Column.* Ph.D. Thesis. Bradford University, Bradford, U.K.; 1988

21. Bahmanyar, H. and Slater M.J. Studies of Drop Break-up in Liquid-liquid Systems in a rotating Disc Contactor. Part 1: Conditions of No Mass Transfer. *Chemical Engineering & Technology.* 1991. 14(2):78-89.

22. Bahmanyar, H. Dean, D.R., Dowling, I.C., Ramlochan, K.M. and Slater M.J. Studies of Drop Break-up in Liquid-liquid Systems in a rotating Disc Contactor.

Part II: Effects of Mass Transfer and Scale-up. *Chemical Engineering & Technology*. 1991. 14(3):178-185.

23. Hinze, J.O. Fundamentals of the Hydrodynamic Mechanism of Splitting in Dispersion Processes. *AICh.E Journal*. 1955. 1(3):289-295.

24. Strand, C. P., Olney, R.B., Ackerman, G.H. Fundamental Aspects of Rotating Disc Contactor Performance. *AICh.E Journal*. 1962. 8(2):252

25. Zhang, S.H., Yu, S.C., Zhou, Y.C. A Model For Liquid-liquid Extraction Column Performance: The Influence of Drop size distribution on extraction Efficiency *Can. J. Chem. Eng.*. 1985. 63:212-226

26. Slater, M. J., Godfrey J.C., Chang-Kakoti D.K., Fei, W.Y., *Drop Sizes and Distribution in Rotating Disc Contactors*. J. Separ. Proc. Tech. 1985:40-48.

27. Chang-Kakoti D.K.,Fei, W.Y., Godfrey, J.C., Slater, M.J. Drop Sizes and Distributions in Rotating Disc Contactors Used for Liquid-liquid Extraction. *J. Sep. Process Technology*. 1985. 6:40-48.

28. Cauwenberg, V. *Hydrodynamics and Physico-Chemical Aspects of Liquid-Liquid Extraction*. Ph.D Thesis. Katholieke University Leuven, Belgium; 1995

29. Coulaloglou, C.A. and Tavlarides, L.L. Description of Interaction Processes in agitated Liquid-liquid Dispersion. *Chem. Eng. Science*. 1977. 32(11):1289-1297.

30. Jares, J. and Prochazka, J. Break-up of Droplets in Karr Reciprocating Plate Extraction Column. *Chem. Eng. Science*. 1987. 42(2):283-292.

31. Bahmanyar, H., Chang-Kakoti D.K., Garro, L., Liang, T.B. and Slater, M.J. Mass Transfer from single Drops in Rotating Disc, Pulsed Sieve Plate and Packed Liquid-liquid Extraction columns *Trans. Institute Chemical Engineers*. 1990. 68A: 74-83

32. Robert, E.T. *Mass Transfer Operation*. Third Edition. USA: McGraw-Hill. 1980.

33. Bailes, P.J., Godfrey, J.C. and Slater, M.J. Liquid-liquid Extraction Test Systems. *Chemical Engineering Res. Des.* 1983. 61: 321-324

34. Slater, M.J. Rate Coefficients in Liquid-liquid Extraction Systems. In: Godfrey, J.C. and Slater, M.J. *Liquid-Liquid Extraction Equipment*. England: J. Wiley and Sons. 48-94; 1994

35. Vermuelen,T. Theory for Irreversible and Constant-Pattern Solid Diffusion. *Industrial and Engineering Chemistry*. 1953. 45(8):1664-1669.

36. Skelland, A.H.P. and Lee, J.M. Drop Size and Continuous Phase Mass Transfer in Agitated Vessels . *American Institute of Chemical Engineers Journal*. 1981. 27(1):99-111.

37. Muhamed, A.H. *Model Peralihan Jisim Diskret Serentak Bagi Resapan Titisan*, Ms. Thesis. Universiti Teknologi Malaysia, Skudai, Malaysia; 2000

38. Carslaw, H.S. and Jaeger, J.C. *Conduction of Heat in Solids*. London: Oxford University Press. 1959

39. Moise, E.E. *Elementary Geometry From An Advanced Standpoint*. Second Edition. USA: Addison-Wesley Publishing Company Inc. 1974.

40. Simmons, G.F. *Introduction to Topology and Modern Analysis*. USA:McGraw-Hill Book Company. 1963.

41. Rudin, W. *Principle of Mathematical Analysis*. Third Edition. USA: McGraw-Hill Book Company. 1976.

APPENDIX A

Geometrical and Physical Properties of RDC Column

Geometrical properties of RDC column	
Number of stages	23
Height of a compartment(m)	0.076
Diameter of rotor disc(m)	0.1015
Diameter of column(m)	0.1520
Diameter of stator ring(m)	0.1110
Rotor speed(rev/s)	4.2

Table A.1: The geometrical properties of the rotating disc contactor (RDC) column.

Physical properties of the system(cumene/isobutyric acid/water)	
Continuous phase:isobutyric acid in water	
Dispersed phase:isobutyric acid in cumene	
Viscosity of continuous phase (kg/ms)	0.100E-2
Viscosity of Dispersed phase (kg/ms)	0.710E-3
Density of continuous phase (kg/ms^3)	0.100E+4
Density of dispersed phase (kg/ms^3)	0.862E+3
Molecular diffusivity in the continuous phase (m^2/s)	0.850E-9
Molecular diffusivity in the dispersed phase (m^2/s)	0.118E-8

Table A.2: The physical properties of the system used.

APPENDIX B

GLOSSARY

A glossary of the acronyms used in the thesis is provided below. The acronyms represents some useful mathematical concepts or terms and the names for some algorithms.

NAME	MEANING
ANN	Artificial Neural Network
BAMT	Boundary Approach of Mass Transfer
BMT	Basic Mass Transfer
EVM	Expected Value Mathod
FL	Fuzzy Logic
IAMT	Initial Approach of Mass Transfer
IBVP	Initial Boundary Value Problem
IP	Inverse Problem
IMDMS	Inverse Multiple Drops MUlti-stage
ISDSS	Inverse Single Drop Single Stage
MIMO	Multiple Input Multiple Output
MISO	Multiple Input Single Output
MTASD	Mass Transfer of a Single Drop
MTMD	Mass Transfer of Multiple Drops
MTSS	Mass Transfer steady State
PCA	Principle Component Analysis

RDC	Rotating Disc Contactor
TQDF	Time-dependent Quadratic Driving Force
S-DMT	Simultaneous Discrete Mass Transfer
UIVI	Updating Initial Value for Next Iteration
UIVS	Updating Initial Value for Next Stage
X-ray CT	X-ray Computed Tomography

APPENDIX C

PAPERS PUBLISHED DURING THE AUTHOR'S CANDIDATURE

From the material in this thesis there are, at the time of submission, papers which have been published, presented or submitted for publication or presentation as following:

Books

P1. Maan, N., Talib, J., Arshad, K.A. and Ahmad, T. Inverse Modeling Of Mass Transfer Process in the RDC Column by Fuzzy Approach. In: Mastorakis, N.E., Manikopoulos, C., Antoniou, G.E., Mladenov, V.M. and Gonos, I.F. *Recent Advances in Intelligent Systems and Signal Processing.* Greece: WSEAS Press. 2003: 348–353

Papers published in journals

P2. Normah Maan, Jamalludin Talib and Khairil Anuar Arshad Use of Neural Network for Modeling of Liquid-liquid Extraction Process in the RDC Column. *Matematika.* 19(1).2003. 15–27

P3. Maan, N., Talib, J., Arshad, K.A. and Ahmad, T. On Determination of Input Parameters of The Mass Transfer Process in the Multiple Stages RDC Column by Fuzzy Approach: Inverse Problem *Matematika.* Vol 20(2): 2004

Papers published in proceedings

P4. Normah Maan, Jamalludin Talib and Khairil Anuar Arshad Mass Transfer Model of a Single Drop in the RDC Column. *Prosiding Simposium Kebangsaan Sains Matematik Ke 10* 2002; 217–227.

P5. Maan, N., Talib, J., Arshad, K.A. and Ahmad, T. Inverse Modeling Of Mass Transfer Process in the RDC Column by Fuzzy Approach. *Proceedings of the 7th WSEAS International Multiconference on Circuits, systems, Communications and Computers*. July 7-10. Corfu, Greece: WSEAS, Paper No. 457-281.

P6. Maan, N., Talib, J., Arshad, K.A. and Ahmad, T. On Inverse Problem of the Mass Transfer Process in the Multiple Stages RDC Column: Fuzzy Approach. *Abstract of the International Conference on Inverse Problem: Modeling and Simulation*. 2004.

P7. Maan, N., Talib, J., Arshad, K.A. and Ahmad, T. On Mass Transfer Process In Multiple Stages RDC Column: Inverse Problem. Presented in the Simposium Kebangsaan Sains Matematik Ke 11, Promenade Hotel, Kota Kinabalu, Sabah Dis 22-24, 2003.